# Jefferson Lab PAC25
## Proposal Cover Sheet

This document must be received by close of business Tuesday,

December 2, 2003 at:

Jefferson Lab
User/International Liaison
Mail Stop 12B
12000 Jefferson Ave.
Newport News, VA
23606

**Experimental Hall:** Hall-A

**Days Requested for Approval:** 26

❒ **Proposal Title:**

Precision Measurement of Longitudinal and Transverse Response Functions of Quasi-Elastic Electron Scattering in the Momentum Transfer Range 0.55 GeV/c < q < 0.9 GeV/c

### Proposal Physics Goals

Indicate any experiments that have physics goals similar to those in your proposal.

**Approved, Conditionally Approved, and/or Deferred Experiment(s) or proposals:**

E01-016

### Contact Person


**Name:** Seonho Choi
**Institution:** Temple University
**Address:** 1900 N. 13th Street, Barton Hall
**Address:** Temple University
**City, State, ZIP/Country:** Philadelphia, PA 19122, USA
**Phone:** 757-269-5947 **Fax:** 561-258-7689
**E-Mail:** choi@jlab.org


**Jefferson Lab Use Only**

Receipt Date:_____

By:_____

# LAB RESOURCES LIST

JLab Proposal No.: _____ Date _____

*(For JLab ULO use only.)*

List below significant resources — both equipment and human — that you are requesting from Jefferson Lab in support of mounting and executing the proposed experiment. Do not include items that will be routinely supplied to all running experiments such as the base equipment for the hall and technical support for routine operation, installation, and maintenance.

**Major Installations** *(either your equip. or new equip. requested from JLab)*

New collimator design/engineer/fab

and installation, if necessary

Target reconfiguration

to have cooling for $^{56}$Fe

*New Support Structures:* _____

***Data Acquisition/Reduction***

*Computing Resources:* _____

*New Software:* _____

**Major Equipment**

Magnets*:* _____

Power Supplies*:* _____

Targets*:* _____

Detectors*:* _____

Electronics*:* _____

Computer Hardware*:* _____

Other*:* _____

**Other:** _____

# BEAM REQUIREMENTS LIST

JLab Proposal No.: _____ Date: _____

Hall: Hall-A Anticipated Run Date: _____ PAC Approved Days: _____

Spokesperson: S. Choi, J.-P. Chen, Z.-E. Meziani Hall Liaison: J.-P. Chen
Phone: 757-269-5947
E-mail: choi@jlab.org

List all combinations of anticipated targets and beam conditions required to execute the experiment. (This list will form the primary basis for the Radiation Safety Assesment Document (RSAD) calculations that must be performed for each experiment.)

| Condition No. | Beam Energy (MeV) | Mean Beam Current (μA) | Polarization and Other Special Requirements (e.g., time structure) | Target Material (use multiple rows for complex targets — e.g., w/windows) | Material Thickness (mg/cm$^2$) | Est. Beam-On Time for Cond. No. (hours) |
|---|---|---|---|---|---|---|
| 1 | 400 | 50 | | $^{4}$He | 1400 | 5.50 |
| 2 | 400 | 50 | | Al | 178.3 | 5.50 |
| 3 | 400 | 50 | | $^{12}$C | 100 | 5.77 |
| 4 | 400 | 50 | | $^{56}$Fe | 100 | 5.50 |
| 5 | 400 | 50 | | $^{208}$Pb | 100 | 5.50 |
| 6 | 500 | 50 | | $^{4}$He | 1400 | 6.33 |
| 7 | 500 | 50 | | Al | 178.3 | 6.33 |
| 8 | 500 | 50 | | $^{12}$C | 100 | 10.38 |
| 9 | 500 | 50 | | $^{56}$Fe | 100 | 6.78 |
| 10 | 500 | 50 | | $^{208}$Pb | 100 | 6.50 |
| 11 | 600 | 50 | | $^{4}$He | 1400 | 8.59 |
| 12 | 600 | 50 | | Al | 178.3 | 8.59 |
| 13 | 600 | 50 | | $^{12}$C | 100 | 16.58 |

The beam energies, $E_{Beam}$, available are: $E_{Beam} = N \times E_{Linac}$ where N = 1, 2, 3, 4, or 5. $E_{Linac}$ = 800 MeV, i.e., available $E_{Beam}$ are 800, 1600, 2400, 3200, and 4000 MeV. Other energies should be arranged with the Hall Leader before listing.

# BEAM REQUIREMENTS LIST

JLab Proposal No.: _____ Date: _____

Hall: Hall-A Anticipated Run Date: _____ PAC Approved Days: _____

Spokesperson: S. Choi, J.-P. Chen, Z.-E. Meziani Hall Liaison: J.-P. Chen
Phone: 757-269-5947
E-mail: choi@jlab.org

List all combinations of anticipated targets and beam conditions required to execute the experiment. (This list will form the primary basis for the Radiation Safety Assesment Document (RSAD) calculations that must be performed for each experiment.)

| Condition No. | Beam Energy (MeV) | Mean Beam Current (μA) | Polarization and Other Special Requirements (e.g., time structure) | Target Material (use multiple rows for complex targets — e.g., w/windows) | Material Thickness (mg/cm$^2$) | Est. Beam-On Time for Cond. No. (hours) |
|---|---|---|---|---|---|---|
| 14 | 600 | 50 | | $^{28}$Fe | 100 | 12.71 |
| 15 | 600 | 50 | | $^{208}$Pb | 100 | 11.05 |
| 16 | 700 | 50 | | $^{4}$He | 1400 | 7.57 |
| 17 | 700 | 50 | | Al | 178.3 | 7.57 |
| 18 | 700 | 50 | | $^{12}$C | 100 | 21.84 |
| 19 | 700 | 50 | | $^{56}$Fe | 100 | 15.36 |
| 20 | 700 | 50 | | $^{208}$Pb | 100 | 12.81 |
| 21 | 800 | 50 | | $^{4}$He | 1400 | 7.97 |
| 22 | 800 | 50 | | Al | 178.3 | 7.97 |
| 23 | 800 | 50 | | $^{12}$C | 100 | 19.80 |
| 24 | 800 | 50 | | $^{56}$Fe | 100 | 13.12 |
| 25 | 800 | 50 | | $^{208}$Pb | 100 | 12.76 |
| 26 | 900 | 50 | | $^{4}$He | 1400 | 6.06 |

The beam energies, $E_{Beam}$, available are: $E_{Beam} = N \times E_{Linac}$ where N = 1, 2, 3, 4, or 5. $E_{Linac}$ = 800 MeV, i.e., available $E_{Beam}$ are 800, 1600, 2400, 3200, and 4000 MeV. Other energies should be arranged with the Hall Leader before listing.

# BEAM REQUIREMENTS LIST

JLab Proposal No.: _____ Date: _____

Hall: Hall-A Anticipated Run Date: _____ PAC Approved Days: _____

Spokesperson: S. Choi, J.-P. Chen, Z.-E. Meziani Hall Liaison: J.-P. Chen
Phone: 757-269-5947
E-mail: choi@jlab.org

List all combinations of anticipated targets and beam conditions required to execute the experiment. (This list will form the primary basis for the Radiation Safety Assesment Document (RSAD) calculations that must be performed for each experiment.)

| Condition No. | Beam Energy (MeV) | Mean Beam Current (μA) | Polarization and Other Special Requirements (e.g., time structure) | Target Material (use multiple rows for complex targets — e.g., w/windows) | Material Thickness (mg/cm$^2$) | Est. Beam-On Time for Cond. No. (hours) |
|---|---|---|---|---|---|---|
| 27 | 900 | 50 | | Al | 178.3 | 6.06 |
| 28 | 900 | 50 | | $^{12}$C | 100 | 17.88 |
| 29 | 900 | 50 | | $^{56}$Fe | 100 | 13.68 |
| 30 | 900 | 50 | | $^{208}$Pb | 100 | 11.18 |
| 31 | 1000 | 50 | | $^{4}$He | 1400 | 2.52 |
| 32 | 1000 | 50 | | Al | 178.3 | 2.52 |
| 33 | 1000 | 50 | | $^{12}$C | 100 | 12.51 |
| 34 | 1000 | 50 | | $^{56}$Fe | 100 | 6.60 |
| 35 | 1000 | 50 | | $^{208}$Pb | 100 | 5.14 |
| 36 | 1100 | 50 | | $^{4}$He | 1400 | 1.88 |
| 37 | 1100 | 50 | | Al | 178.3 | 1.88 |
| 38 | 1100 | 50 | | $^{12}$C | 100 | 6.87 |
| 39 | 1100 | 50 | | $^{56}$Fe | 100 | 5.72 |

The beam energies, $E_{Beam}$, available are: $E_{Beam} = N \times E_{Linac}$ where N = 1, 2, 3, 4, or 5. $E_{Linac}$ = 800 MeV, i.e., available $E_{Beam}$ are 800, 1600, 2400, 3200, and 4000 MeV. Other energies should be arranged with the Hall Leader before listing.

# BEAM REQUIREMENTS LIST

JLab Proposal No.: _____ Date: _____

Hall: Hall-A Anticipated Run Date: _____ PAC Approved Days: _____

Spokesperson: S. Choi, J.-P. Chen, Z.-E. Meziani Hall Liaison: J.-P. Chen
Phone: 757-269-5947
E-mail: choi@jlab.org

List all combinations of anticipated targets and beam conditions required to execute the experiment. (This list will form the primary basis for the Radiation Safety Assesment Document (RSAD) calculations that must be performed for each experiment.)

| Condition No. | Beam Energy (MeV) | Mean Beam Current (μA) | Polarization and Other Special Requirements (e.g., time structure) | Target Material (use multiple rows for complex targets — e.g., w/windows) | Material Thickness (mg/cm$^2$) | Est. Beam-On Time for Cond. No. (hours) |
|---|---|---|---|---|---|---|
| 40 | 1100 | 50 | | $^{208}$Pb | 100 | 3.88 |
| 41 | 1200 | 50 | | $^{4}$He | 1400 | 3.13 |
| 42 | 1200 | 50 | | Al | 178.3 | 3.13 |
| 43 | 1200 | 50 | | $^{12}$C | 100 | 7.60 |
| 44 | 1200 | 50 | | $^{56}$Fe | 100 | 6.21 |
| 45 | 1200 | 50 | | $^{208}$Pb | 100 | 7.24 |
| 46 | 1600 | 50 | | $^{4}$He | 1400 | 0.67 |
| 47 | 1600 | 50 | | Al | 178.3 | 0.67 |
| 48 | 1600 | 50 | | $^{12}$C | 100 | 0.67 |
| 49 | 1600 | 50 | | $^{56}$Fe | 100 | 0.67 |
| 50 | 1600 | 50 | | $^{208}$Pb | 100 | 0.67 |
| 51 | 2000 | 50 | | $^{4}$He | 1400 | 0.50 |
| 52 | 2000 | 50 | | Al | 178.3 | 0.50 |

The beam energies, $E_{Beam}$, available are: $E_{Beam} = N \times E_{Linac}$ where N = 1, 2, 3, 4, or 5. $E_{Linac}$ = 800 MeV, i.e., available $E_{Beam}$ are 800, 1600, 2400, 3200, and 4000 MeV. Other energies should be arranged with the Hall Leader before listing.

# BEAM REQUIREMENTS LIST

JLab Proposal No.: _____ Date: _____

Hall: Hall-A Anticipated Run Date: _____ PAC Approved Days: _____

Spokesperson: S. Choi, J.-P. Chen, Z.-E. Meziani Hall Liaison: J.-P. Chen
Phone: 757-269-5947
E-mail: choi@jlab.org

List all combinations of anticipated targets and beam conditions required to execute the experiment. (This list will form the primary basis for the Radiation Safety Assesment Document (RSAD) calculations that must be performed for each experiment.)

| Condition No. | Beam Energy (MeV) | Mean Beam Current (μA) | Polarization and Other Special Requirements (e.g., time structure) | Target Material (use multiple rows for complex targets — e.g., w/windows) | Material Thickness (mg/cm$^2$) | Est. Beam-On Time for Cond. No. (hours) |
|---|---|---|---|---|---|---|
| 53 | 2000 | 50 | | $^{12}$C | 100 | 0.50 |
| 54 | 2000 | 50 | | $^{56}$Fe | 100 | 0.50 |
| 55 | 2000 | 50 | | $^{208}$Pb | 100 | 0.50 |
| 56 | 2400 | 50 | | $^{4}$He | 1400 | 0.50 |
| 57 | 2400 | 50 | | Al | 178.3 | 0.50 |
| 58 | 2400 | 50 | | $^{12}$C | 100 | 0.50 |
| 59 | 2400 | 50 | | $^{56}$Fe | 100 | 0.50 |
| 60 | 2400 | 50 | | $^{208}$Pb | 100 | 0.50 |
| 61 | 2800 | 50 | | $^{4}$He | 1400 | 0.50 |
| 62 | 2800 | 50 | | Al | 178.3 | 0.50 |
| 63 | 2800 | 50 | | $^{12}$C | 100 | 0.50 |
| 64 | 2800 | 50 | | $^{56}$Fe | 100 | 0.50 |
| 65 | 2800 | 50 | | $^{208}$Pb | 100 | 0.50 |

The beam energies, $E_{Beam}$, available are: $E_{Beam} = N \times E_{Linac}$ where N = 1, 2, 3, 4, or 5. $E_{Linac}$ = 800 MeV, i.e., available $E_{Beam}$ are 800, 1600, 2400, 3200, and 4000 MeV. Other energies should be arranged with the Hall Leader before listing.

# BEAM REQUIREMENTS LIST

JLab Proposal No.: _____ Date: _____

Hall: Hall-A Anticipated Run Date: _____ PAC Approved Days: _____

Spokesperson: S. Choi, J.-P. Chen, Z.-E. Meziani Hall Liaison: J.-P. Chen
Phone: 757-269-5947
E-mail: choi@jlab.org

List all combinations of anticipated targets and beam conditions required to execute the experiment. (This list will form the primary basis for the Radiation Safety Assesment Document (RSAD) calculations that must be performed for each experiment.)

| Condition No. | Beam Energy (MeV) | Mean Beam Current (μA) | Polarization and Other Special Requirements (e.g., time structure) | Target Material (use multiple rows for complex targets — e.g., w/windows) | Material Thickness (mg/cm$^2$) | Est. Beam-On Time for Cond. No. (hours) |
|---|---|---|---|---|---|---|
| 66 | 3200 | 50 | | $^{4}$He | 1400 | 0.66 |
| 67 | 3200 | 50 | | Al | 178.3 | 0.66 |
| 68 | 3200 | 50 | | $^{12}$C | 100 | 0.50 |
| 69 | 3200 | 50 | | $^{56}$Fe | 100 | 0.50 |
| 70 | 3200 | 50 | | $^{208}$Pb | 100 | 0.50 |
| 71 | 3600 | 50 | | $^{4}$He | 1400 | 0.69 |
| 72 | 3600 | 50 | | Al | 178.3 | 0.69 |
| 73 | 3600 | 50 | | $^{12}$C | 100 | 0.40 |
| 74 | 3600 | 50 | | $^{56}$Fe | 100 | 0.33 |
| 75 | 3600 | 50 | | $^{208}$Pb | 100 | 0.33 |
| | | | | | | |
| | | | | | | |
| | | | | | | |

The beam energies, $E_{Beam}$, available are: $E_{Beam} = N \times E_{Linac}$ where N = 1, 2, 3, 4, or 5. $E_{Linac}$ = 800 MeV, i.e., available $E_{Beam}$ are 800, 1600, 2400, 3200, and 4000 MeV. Other energies should be arranged with the Hall Leader before listing.

# HAZARD IDENTIFICATION CHECKLIST

JLab Proposal No.: _____ Date: _____
(For CEBAF User Liaison Office use only.)

Check all items for which there is an anticipated need.

**Cryogenics**
- __X__ beamline magnets
- __X__ analysis magnets
- __X__ target
  - type: _____
  - flow rate: _____
  - capacity: _____

**Electrical Equipment**
- __X__ cryo/electrical devices
- _____ capacitor banks
- __X__ high voltage
- _____ exposed equipment

**Radioactive/Hazardous Materials**
List any radioactive or hazadorous/ toxic materials planned for use:
_____
_____
_____
_____

**Pressure Vessels**
- _____ inside diameter
- _____ operating pressure
- _____ window material
- _____ window thickness

**Flammable Gas or Liquids**
- type: _____
- flow rate: _____
- capacity: _____

**Drift Chambers**
- type: Ethene/Argonne (50/50)
- flow rate: 7 *l*/hr × 4 chambers
- capacity: 30 *l* × 4 chambers

**Other Target Materials**
- ___ Beryllium (Be)
- ___ Lithium (Li)
- ___ Mercury (Hg)
- __X__ Lead (Pb)
- ___ Tungsten (W)
- ___ Uranium (U)
- ___ Other (list below)

_____
_____

**Vacuum Vessels**
- _____ inside diameter
- _____ operating pressure
- _____ window material
- _____ window thickness

**Radioactive Sources**
- _____ permanent installation
- _____ temporary use
- type: _____
- strength: _____

**Large Mech. Structure/System**
- _____ lifting devices
- _____ motion controllers
- _____ scaffolding or
- _____ elevated platforms

**Lasers**
- type: _____
- wattage: _____
- class: _____

Installation:
- _____ permanent
- _____ temporary

Use:
- _____ calibration
- _____ alignment

**Hazardous Materials**
- ____ cyanide plating materials
- ____ scintillation oil (from)
- ____ PCBs
- ____ methane
- ____ TMAE
- ____ TEA
- ____ photographic developers
- ____ other (list below)

_____
_____

**General:**

Experiment Class:

- _____ Base Equipment
- _____ Temp. Mod. to Base Equip.
- _____ Permanent Mod. to Base Equipment
- _____ Major New Apparatus

Other: _____
_____

# Computing Requirements List

**Proposal Title:** Precision Measurement of Longitudinal and Transverse Response Functions of Quasi-Elastic Electron Scattering in the Momentum Transfer Range 0.55 GeV/$c$ < |**q**| < 0.9 GeV/$c$

**Spokesperson:** S. Choi, J.-P. Chen, Z.-E. Meziani **Experimental Hall:** Hall-A

**Raw Data Expected**

**Total:** 2.5TB **Per Year (long duration experiments only):** _____

**Simulation Compute Power (SPECint95 hours) Required:** 2000 Hours

**On-Line Disk Storage Required:** 50GB

**Imported Data Amount from Outside Institutions:** _____

**Exported Data Amount to Outside Institutions:w** _____

**Expected Mechanism for Imported/Exported Data:** _____

## Special Requirements

**For example, special configuration of data acquisition systems) that may require resources and/or coordination with JLab's Computer Center. Please indicate, if possible, what fraction of these resources will be provided by collaborating institutions and how much is expected to be provided by JLab.**

# Precision Measurement of Longitudinal and Transverse Response Functions of Quasi-Elastic Electron Scattering in the Momentum Transfer Range $0.55\ \mathrm{GeV}/c \leq |\mathbf{q}| \leq 0.9\ \mathrm{GeV}/c$


J. Morgenstern
*CEA Saclay DSM/DAPNIA/SPhN F91191, Gif-sur-Yvette Cedex, France*

J. Templon
*University of Georgia, Athens, GA 30602*

J.-P. Chen (Co-spokesperson), E. Chudakov, R. Feuerbach, C. W. de Jager, M. Jones, J. Gomez, J.-O. Hansen, D.W. Higinbotham, J. LeRose, R. Michaels, B. Reitz, A. Saha, B. Wojtsekhowski
*Jefferson Lab, Newport News, VA 23606*

A. Adeluyi, A. T Katramatou, G. G. Petratos
*Kent State University, Kent, OH 44242*

W. Korsch
*University of Kentucky, Lexington, KY 40506*

W. Bertozzi, S. Gilad, S. Sirca, R. Suleiman
*Massachusetts Institute of Technology, Cambridge, MA 02139, USA*

F. Benmokhtar, R. Gilman, C. Glashausser, X. Jiang, G. Kumbartzki, K. McCormick, R. Ransome, J. Yuan
*Rutgers University, Piscataway, NJ 08855*

Seonho Choi (Spokesperson), F. Butaru, A. Lukhanin,
Z.-E. Meziani (Co-spokesperson), K. Slifer, P. Solvignon, H. Yao
*Temple University, Philadelphia, PA 19122*

N. Liyanage
*University of Virginia, Charlottesville, VA 22901*

T. Averett, T. Holmstrom, V. Sulkosky
*College of William and Mary, Williamsburg, VA 23185*

and

Hall A Collaboration

Contact: Seonho Choi (choi@jlab.org)

December 2, 2003

**Abstract**

We propose to make a precision measurement of inclusive electron scattering cross sections in the quasi-elastic region for a wide range of momentum transfers for $^{4}$He, $^{12}$C, $^{56}$Fe and $^{208}$Pb. We will extract the longitudinal and transverse response functions in the momentum transfer range $0.55\ \mathrm{GeV}/c \leq |\mathbf{q}| \leq 0.9\ \mathrm{GeV}/c$ with a precision of a few percent improving significantly on the precision of previous measurements in the overlap region. This should allow us to confirm/refute the presently controversial issue of the quenching of the longitudinal response function in medium weight nuclei and as importantly investigate the $|\mathbf{q}|$ evolution of the Coulomb Sum Rule as we probe significantly shorter distances.

# 1 Introduction

The JLab proposal E01-016, entitled "Precision Measurement of Longitudinal and Transverse Response Functions of Quasi-Elastic Electron Scattering in the Momentum Transfer Range $0.55\ \mathrm{GeV}/c \leq |\mathbf{q}| \leq 1.0\ \mathrm{GeV}/c$" was approved by PAC19 for 26 days with "A-" rating. Since the experiment has not been run or scheduled for the last three years, it is returning to the new PAC as a jeopardy proposal. We are providing an update composed of

- a brief summary of the original proposal, JLab E01-016
- study of the spectrometer background using a newly developed simulation program
- the one page PAC19 report on the original proposal
- a copy of the original proposal.

In the original proposal, we aimed to cover $|\mathbf{q}|$ up to 1.0 GeV/$c$. But following the PAC19 suggestion to leave out the data at the highest $|\mathbf{q}|$ values, in this update, we will limit the maximum $|\mathbf{q}|$ value to 0.9 GeV/$c$.

# 2 Brief Summary of JLab Proposal E01-016

One of the important questions in nuclear physics is how nucleon properties are affected by the nuclear medium, since it might form a bridge from the strong interaction between nucleons to the underlying theory of Quantum ChromoDynamics (QCD). Since elastic scattering of electrons from a free nucleon has been well measured, quasi-elastic electron scattering off nuclei is a promising tool to investigate the properties of nucleons in nuclei. In particular, a Rosenbluth separation of the charge and magnetic responses of a nucleus can test a model-independent property known as the Coulomb Sum Rule (CSR).

This sum rule states that when integrating the charge response of a nucleus over the full range of energy loss $\omega$ at large enough three-momentum transfer $|\mathbf{q}|$, one should count the number of protons ($Z$) in a nucleus. This simple picture can be spoiled by a modification of the free nucleon electromagnetic properties in the nuclear medium and the presence of nucleon-nucleon short-range correlations. However, it is expected that around the momentum transfer of 550 MeV/$c$, the CSR should not deviate by more than a few percent due to $N - N$ correlations,

and reach saturation at higher momentum transfer, independent of the $N-N$ force chosen. Thus a deviation from the CSR in the range $|\mathbf{q}| \simeq 550$ MeV/$c$ might indicate a possible modification of the nucleon electric properties in the nuclear medium.

In the last twenty years, a large experimental program has been carried out at Bates, Saclay and SLAC aimed at the extraction of these two response functions for a variety of nuclei from $^4$He to $^{208}$Pb. Overall consistency of the data set between different laboratories has been observed except for $^{40}$Ca. And in the case of medium-weight and heavy nuclei, conclusions reached by different experiments ranged from a full saturation of the CSR to its violation by 30%. Furthermore, a recent analysis [1, 2] argued that the "so-called quenching is mostly due to the limited significance of the data" and that including data at high energy loss $\omega$ leads to the result that "no $A$-dependent quenching is observed."

In a new analysis [3], it was argued that if one uses the effective momentum approximation (EMA) for performing the Coulomb corrections (as supported by $e^+/e^-$ data to theory comparisons), the quenching still persists even when the world data were included. It was pointed out that consistency among different data sets is observed when the Coulomb corrections were included using the EMA. Figure 1 shows the results obtained for $S_L$ of $^{40}$Ca, $^{48}$Ca, $^{56}$Fe and $^{208}$Pb in this new analysis[3]. The results are compared to theoretical calculations for nuclear matter [4] (solid black curve) and $^4$He [5] (dashed curve); the results in these two cases as expected are very similar and exhibit only a few percent quenching beyond $q_{eff} \sim 500$ MeV/c. The experimental results are to be compared with the long-dashed curve which corresponds to the same calculations as the solid curve but integrated within the experimental limits of excitation energy $\omega$. A quenching of between 20% and 30% in medium weight nuclei persists.

Kinematics covers the momentum transfer range $0.55\,\mathrm{GeV}/c \leq |\mathbf{q}| \leq 0.9\,\mathrm{GeV}/c$ with the beam energies ranging from 400 MeV to 3.6 GeV. For a Rosenbluth separation of longitudinal response function $R_L$, we chose four scattering angles: 15°, 60°, 90° and 120°. The minimum number of necessary angles for a Rosenbluth separation is two. However, having additional angles enables us to check for any angle dependent systematic errors and the linearity of the Rosenbluth plot. The uncertainty on the spectrometer angle can be reduced to 0.2 mrad with additional calibration data at each angle, as shown in [7]. With this choice of kinematics, at each $|\mathbf{q}|$, the excitation energy range covers the quasi-elastic peak and part of $\Delta$-resonance where $R_L$ is expected to be small or close to zero[8].

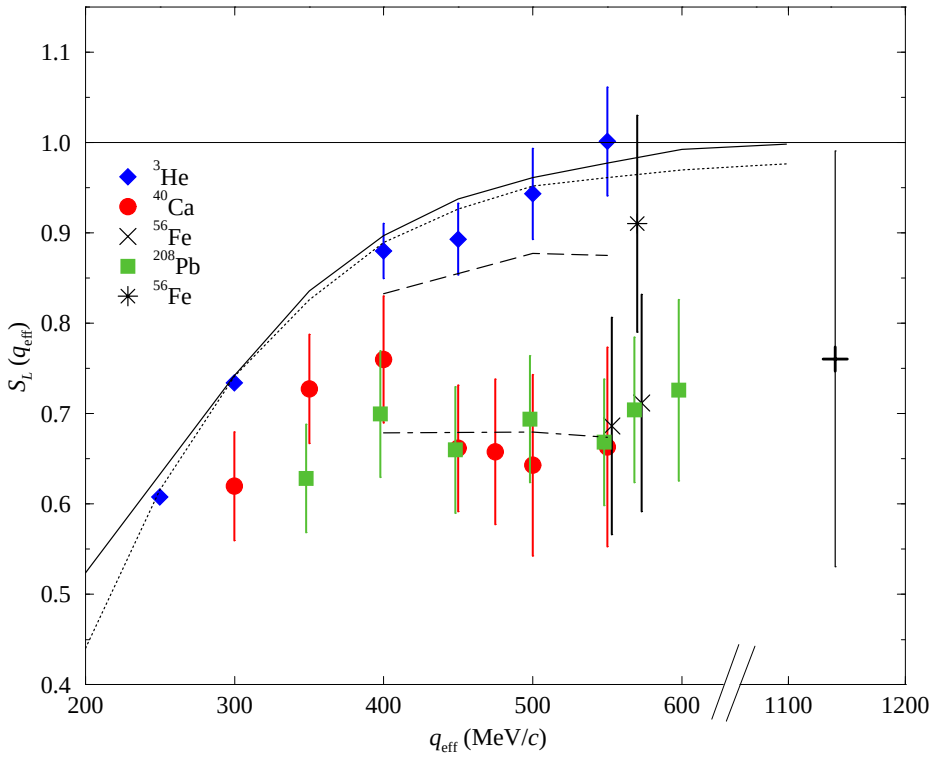


Figure 1: $S_L$ obtained in the EMA as a function of $q_{eff}$ using Saclay data combined with SLAC NE3 and Bates. The $^{56}$Fe SLAC NE9 result [6] (right cross) and that of [1, 2] (star) are also shown.

We will use four different targets, $^4$He, $^{12}$C, $^{56}$Fe and $^{208}$Pb with beam current up to 50$\mu$A. The two spectrometers of Hall-A will do independent measurements at a given beam energy and we shall optimize the angle settings to minimize the overhead of momentum and angle change. The estimated systematic uncertainty is 1.7% for the solid targets and 2.2% for the gas target. The final estimate of systematic uncertainties are plotted on Figure 2.

# 3 Study of Spectrometer Background

One of the issues raised by the PAC19 is the experimental backgrounds. In response to their suggestions, we started to address the background issues by simulations, analysis of existing data and new, dedicated tests to study the background.

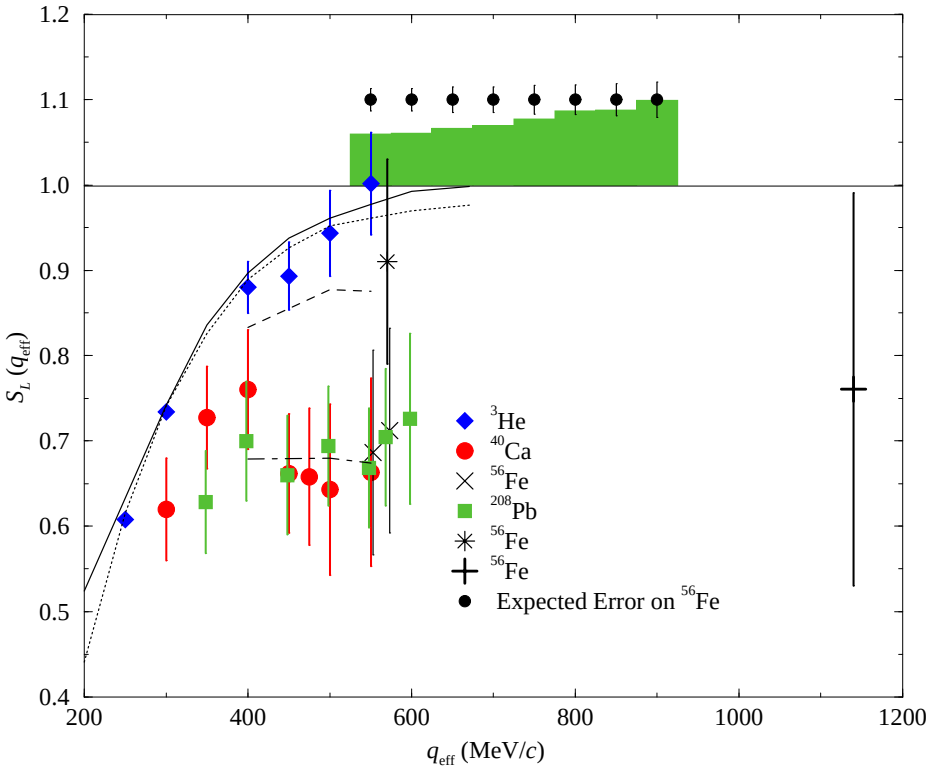


Figure 2: Comparison of expected statistical uncertainty on the Coulomb Sum from Jefferson Lab with the world data. Horizontal band represents estimated systematic uncertainties.

This section presents the result of the simulations.

We have studied the background generated by the interaction of electrons with inside materials of the spectrometer using a Monte-Carlo simulation. The simulation is based on one of the Hall-A simulation programs, SNAKE. In the original version of SNAKE, the electrons hitting internal boundaries of the spectrometer were considered lost. But in our modified new version of the simulation program, those electrons undergo a GEANT simulation for one of two possibilities of

- a single, large angle scattering on the surface, a process analogous to bouncing off the surface, or
- generation of secondary particles from interactions inside the surface material.

Then these bounced-off-electrons or secondary particles were re-inserted into the SNAKE simulation to be traced to the focal plane.

Since no major loss of electrons was found on the pole tips of the dipole magnet in earlier SNAKE simulations, we have focused on the interaction of electrons in the Q3 magnet. Intuitively, due to the proximity of the Q3 magnet to the focal plane, electrons bouncing off the surface of the Q3 magnet would have a higher probability of survival.

The result of the simulation shows that the background generated in this process is about 2% of the clean events at a spectrometer momentum setting of 1.0 GeV/$c$. We find that the ratio decreases to 1.4% at a momentum setting of 0.1 GeV/$c$, the lowest momentum setting among our proposed kinematics.

Figures 3 and 4 show the energy distribution of clean events and background events for two different spectrometer momentum settings, 0.1 GeV/$c$ and 1.0 GeV/$c$. As shown in Figure 3 and Figure 4, most of the background events are low energy secondary particles. A few background events with energy comparable to clean events are coming from a single, large angle scattering on the surface of the Q3 magnet.

As Figure 5 shows, these background events cover a much wider area in the focal plane than clean events with almost uniform distribution. With a conservative cut on the position on the focal plane, about 80% of the background events were eliminated (83% at 0.1 GeV/c momentum setting and 85% at 1.0 GeV/c momentum setting). This result is in agreement with an independent analysis [12], where it was suggested that most of such background can be eliminated by tracing back VDC tracks to the Q3 magnet.

The remaining background events after focal plane position cut can be eliminated by an independent energy measurement such as calorimeter used in the DVCS experiment. The DVCS calorimeter is composed of 132 blocks of $PbF_2$ of size $3\times3\times18.6$ cm$^3$. Arranged in $6\times22$ array, it will cover an area of $18\times66$ cm$^2$ which is roughly 18% of the focal plane ($36\times180$ cm$^2$). We will add additional blocks to cover $18\times132$ cm$^2$. By placing calorimeter around the center of the focal plane, we can maximize the acceptance. Furthermore, the events on the edges of the focal plane will be cut out to remove the background events, so the loss of the acceptance by not covering the whole focal plane is not significant. This type of calorimeter has an energy resolution of $3\%/\sqrt{E}$ and is enough to cut out 96% of the low energy background at 0.1 GeV/$c$ momentum setting (98% at 1.0 GeV/$c$ configuration).

From this study, it was found that up to 2% of background events can be generated by reflection on the Q3 magnet. However, we have shown that this type

of background can be reduced significantly by

- a cut on focal plane position and angle from the VDC tracking information
- and an independent energy measurement using calorimeters.

As mentioned earlier, the current version of the simulation program does not include any pole-tip reflections from other magnets (especially dipole magnet). We are in the process of implementing reflection from other surfaces along the path of the electron and the result will be available by the PAC presentation.

The results of the simulation will be further corroborated by the analysis of existing data and dedicated measurements in the future. Currently, we don't see any significant benefit of putting an additional collimator (active or passive) inside the magnets. If future tests show significant amount of background from other sources, we will consider various options including collimator to reduce the background level.

# 4 Coulomb Distortions

The PAC19 has also suggested to seek close collaboration with theorists to resolve the issues involving the Coulomb distortions. We have contacted a number of theorists to address this issue and a number of theoretical papers[9, 10, 11] were published recently. Theortical activities are on-going and are expected to intensify once the experiment is scheduled.

Recently, another QED correction, namely the two-photon exchange correction, has received special attention. This is in relation to the discrepancy observed between the determination of the ratio of the electric to magnetic proton form factors by Rosenbluth separations compared to the determination of the same ratio by means of polarization measurement of the knock-out proton in elastic scattering. It was proposed that the two-photon exchange correction, although small in absolute value has a variation as a function of the virtual photon polarization. This would have an impact on the Rosenbluth method but not on the polarization measurement method. Our best estimate in the range $|\mathbf{q}| \simeq 1$ GeV/$c$ shows that this effect is small in our case[13, 14].

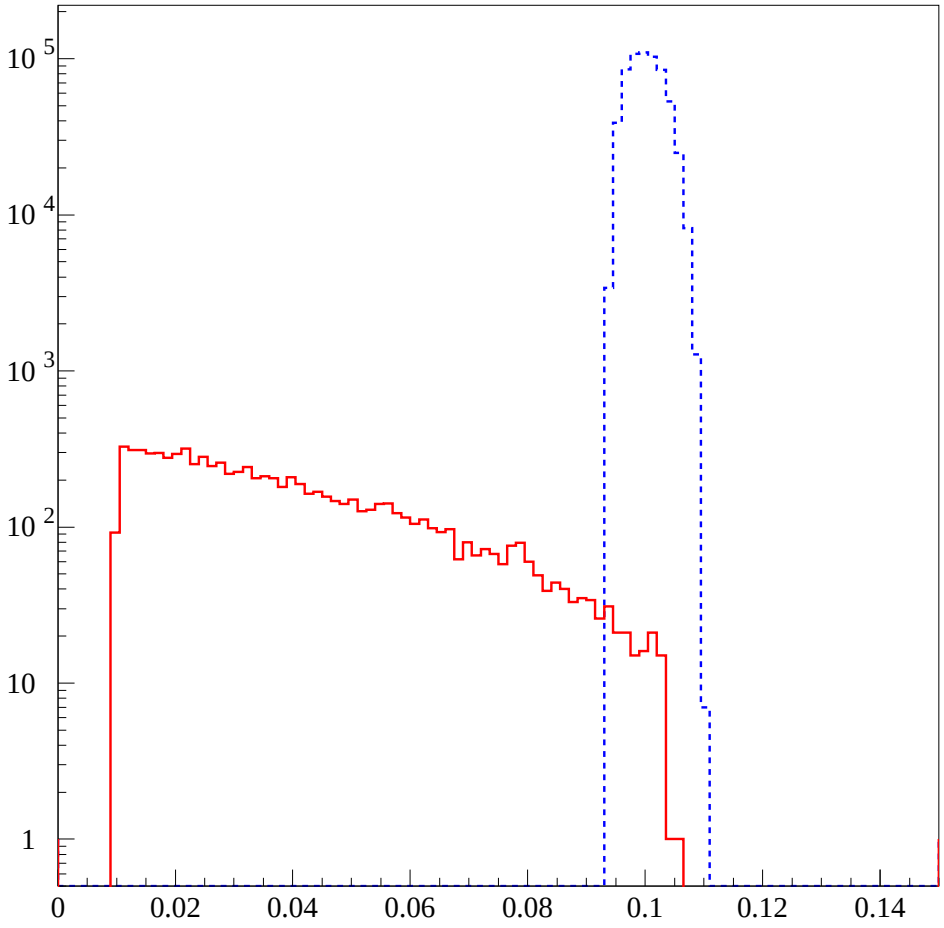


Figure 3: Energy distribution of clean events (blue dashed line) and background events (red solid line) at spectrometer momentum setting of 0.1 GeV/$c$.

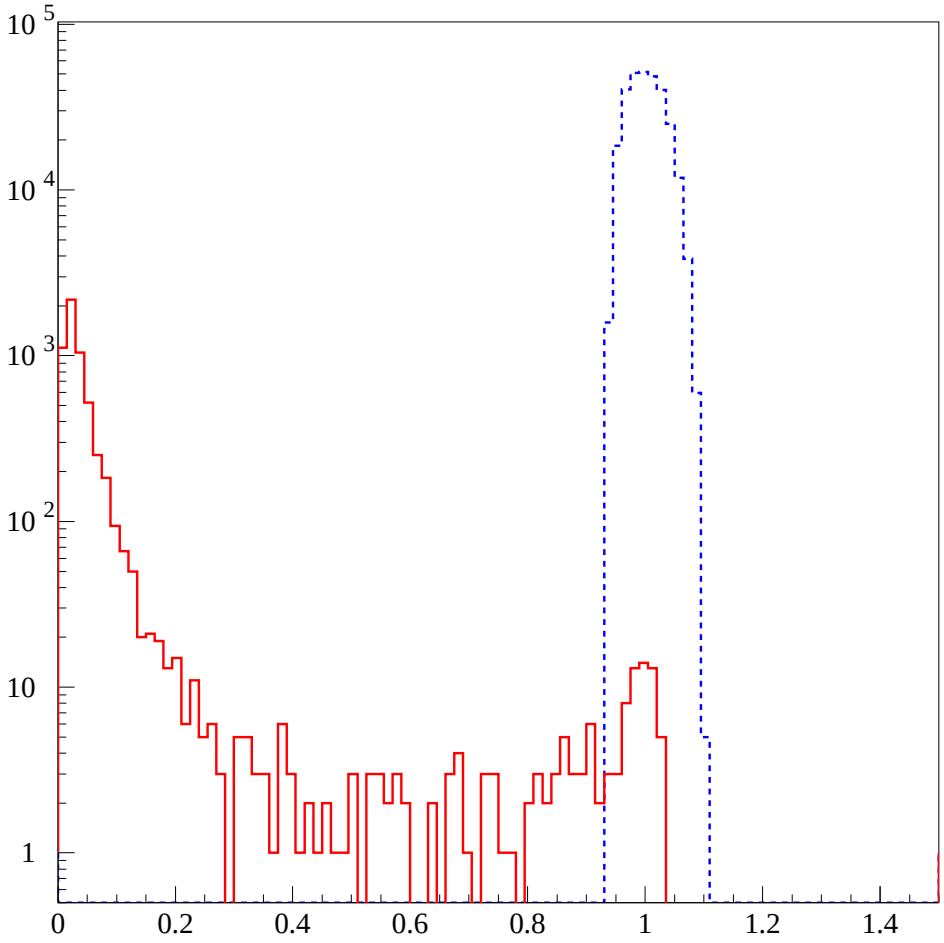


Figure 4: Energy distribution of clean events (blue dashed line) and background events (red solid line) at spectrometer momentum setting of 1.0 GeV/$c$.

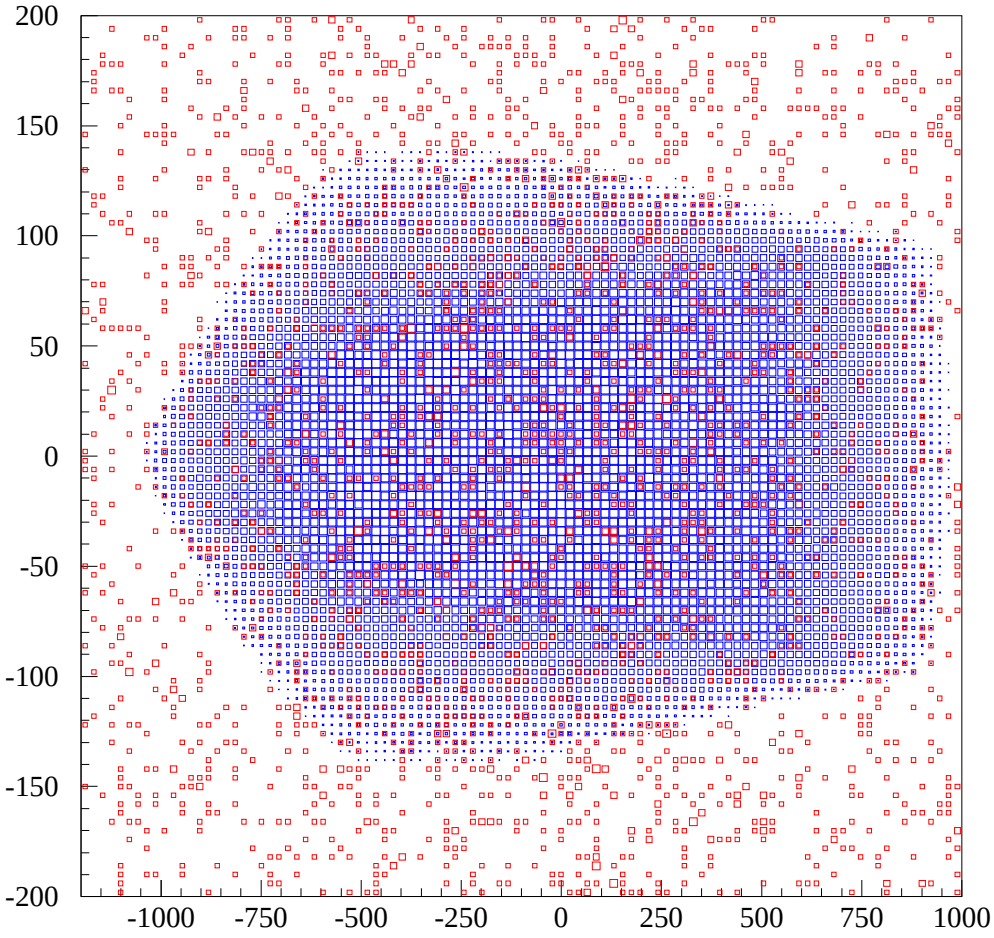


Figure 5: Distribution in focal plane of clean events (blue boxes) and background events (red boxes) at spectrometer momentum setting of 0.1 GeV/$c$. Actually, the background events have much wider distribution outside of the plot which are not shown here.

# References


[1] J. Jourdan, Phys. Lett. **353B**, 189 (1995).

[2] J. Jourdan, Nucl. Phys. **A603**, 117 (1996).

[3] J. Morgenstern and Z.-E. Meziani, Phys. Lett. **B515**, 269 (2001).

[4] A. Fabrocini and S. Fantoni, Nucl. Phys. A **503**, 375 (1989).

[5] R. Schiavilla *et al.*, Nucl. Phys. A **499**, 301 (1989).

[6] J. P. Chen *et al.*, Phys. Rev. Lett. **66**, 1283 (1991).

[7] Paul E. Ulmer, Hassan Ibrahim and Nilanga Liyanage, JLab Technical Note, JLAB-TN-00-024 (2000).

[8] D. T. Baran *et al.*, Phys. Rev. Lett. **61**, 400 (1988).

[9] M. Traini, Nucl. Phys. A **694**, 325 (2001).

[10] K. S. Kim and L. E. Wright, Phys. Rev. C **67**, 054604 (2003).

[11] K. S. Kim and L. E. Wright, Phys. Rev. C **68**, 027601 (2003).

[12] J. Arrington, presentation given at JLab E01-001 collaboration meeting (2003).

[13] P. A. M. Guichon and M. Vanderhaeghen, Phys. Rev. Lett. **91**, 142303 (2003).

[14] P. G. Blunden, W. Melnitchouk and J. A. Tjon, Phys. Rev. Lett. **91**, 142304 (2003).

# Individual Proposal Report

**Proposal: E-**01-016

**Scientific Rating:** $A^-$

**Title:** Precision Measurement of Longitudinal and Transverse Response Functions of Quasi-Elastic Electron Scattering in the Momentum Transfer Range 0.55 GeV/c < q < 1.0 GeV/c.

**Spokespersons:** Seonho Choi, J.-P. Chen and Z.-E. Meziani

**Motivation**: The q-dependence of the integral over the energy transfer,$\omega$ , of the longitudinal response function $R_L$ in quasi-elastic scattering from nuclei, known as the Coulomb sum rule, can yield information on nucleon-nucleon correlations and possible modifications of nucleon properties in a nucleus. Existing data for $R_L$ do not extend beyond q=600 MeV/c and sometimes scatter widely. The goal of the proposal is to obtain a consistent and accurate data set for the nuclei $^4$He, C, Fe and Pb, in order to get a definitive answer on the evolution of the Coulomb sum rule as a function of q up to a q-value of 1.0 GeV/c.

**Measurement and Feasibility:** Values for $R_L$ are obtained by performing a Rosenbluth separation of cross sections obtained at the same value of q and $\omega$ for different values of the polarization parameter, $\varepsilon$. In previous experiments, most of which were done at accelerators with maximum energies below 1 GeV, the range in $\varepsilon$ was limited and the maximum value of q was about 600 MeV/c. In the proposed experiment the range in $\varepsilon$ will be as large as 0.85 and the data can be extended up to a value q=1.0 GeV/c. Interpolation uncertainties and uncertainties in the radiative corrections will be minimized by taking data for a well covered range in q. Data will be obtained at four $\varepsilon$ points in order to check systematic uncertainties in the Rosenbluth separation. Different ways to treat the Coulomb corrections for the heavier nuclei lead at this moment to rather different results.

**Issues:** The PAC recognizes the importance of performing a definitive study of the Coulomb sum rule. The quality of the CEBAF beams and experimental equipment should allow that. In the past some data sets have been plagued by experimental backgrounds. These should be studied carefully, using all possible means. Also one should perform checks with the $^1$H(e,e'p) reaction for every choice of kinematics. Given the increase in the anticipated (systematic) uncertainties at increasing values of q, and the expected flattening of the sum rule at high q, the PAC recommends leaving out the data at the highest q values. It is also suggested to seek close collaboration with theorists to resolve the issues involving the Coulomb distortions.

**Recommendation:** Approve for 26 days in Hall A.

# Precision Measurement of Longitudinal and Transverse Response Functions of Quasi-Elastic Electron Scattering in the Momentum Transfer Range $0.55\ \mathrm{GeV}/c \leq |\mathbf{q}| \leq 1.0\ \mathrm{GeV}/c$


J. Morgenstern
*CEA Saclay DSM/DAPNIA/SPhN F91191, Gif-sur-Yvette Cedex, France*

J. Templon
*University of Georgia, Athens, GA 30602*

J.-P. Chen (Co-spokesperson), E. Chudakov, C. W. de Jager, M. Jones, J. Gomez, J.-O. Hansen, J. LeRose, N. Liyanage, R. Michaels, J. Mitchell, A. Saha, B. Wojtsekhowski
*Jefferson Lab, Newport News, VA 23606*

A.T Katramatou, K. McCormick, G.G. Petratos
*Kent State University, Kent, OH 44242*

W. Korsch, P. Zolnierczuk
*University of Kentucky, Lexington, KY 40506*

W. Bertozzi, S. Gilad, D.W. Higinbotham, S. Sirca, R. Suleiman, Z. Zhou
*Massachusetts Institute of Technology, Cambridge, MA 02139, USA*

F. Benmokhtar, S. Dieterich, R. Gilman, C. Glashausser, X. Jiang, G. Kumbartzki, R. Ransome, S. Strauch
*Rutgers University, Piscataway, NJ 08855*

Seonho Choi (Spokesperson), A. Lukhanin, Z.-E. Meziani (Co-spokesperson),
K. Slifer, P. Solvignon, J. Shousky
*Temple University, Philadelphia, PA 19122*

T. Averett
*College of William and Mary, Williamsburg, VA 23185*

and

Hall A Collaboration

Contact: Seonho Choi (choi@jlab.org)

December 1, 2003

**Abstract**

We propose to make a precision measurement of inclusive electron scattering cross sections in the quasi-elastic region for a wide range of momentum transfers for $^{4}$He, $^{12}$C, $^{56}$Fe and $^{208}$Pb. We will extract the longitudinal and transverse response functions in the momentum transfer range $0.55\ \mathrm{GeV}/c \leq |\mathbf{q}| \leq 1.0\ \mathrm{GeV}/c$ with a precision of a few percent improving significantly on the precision of previous measurements in the overlap region. This should allow us to confirm/refute the presently controversial issue of the quenching of the longitudinal response function in medium weight nuclei and as importantly investigate the $|\mathbf{q}|$ evolution of the Coulomb Sum Rule as we probe significantly shorter distances.

# 1 Introduction and Motivation

One of the important questions in nuclear physics is how nucleon properties are affected by the nuclear medium, since it might form a bridge between the strong interaction between nucleons and the underlying theory of Quantum ChromoDynamics (QCD). A good example is the partial restoration of chiral symmetry in nuclear matter and its consequence for nucleon properties in the nuclear medium (for a comprehensive review see Ref. [1]). Since elastic scattering from a free nucleon has been well measured, quasi-elastic electron scattering off nuclei is considered a promising tool to investigate the properties of nucleons in nuclei. In particular, it was proposed [2] that a Rosenbluth separation of the charge and magnetic responses of a nucleus ($R_L$ and $R_T$, respectively) could test a model-independent property known as the Coulomb sum rule (CSR). This sum rule states that when integrating the quasi-elastic $R_L(q,\omega)$ over the full range of energy loss $\omega$ at large enough three-momentum transfer $|\mathbf{q}| = q$ (greater than twice the Fermi momentum, $q \geq 500$ MeV/c), one should count the number of protons (Z) in a nucleus. More explicitly the quantity $S_L(q)$ defined by

$$S_L(q) = \frac{1}{Z}\int_{0^+}^{\infty} \frac{R_L(q,\omega)}{\tilde{G_E}^2} d\omega$$

is predicted to be unity in the limit of large $q$. Here $\tilde{G_E} = (G_E^p + N/ZG_E^n)\zeta$ takes into account the nucleon charge form factor inside the nucleus (which is usually taken to be equal to that of a free nucleon) as well as a relativistic correction ($\zeta$) suggested by de Forest [3]. The lower limit of integration $0^+$ excludes the elastic peak and the excited states of the nucleus.

This simple picture can be spoiled by the modification of the free nucleon electromagnetic properties by the nuclear medium and the presence of nucleon-nucleon short-range correlations. However, it is expected that around $q$ of 500 MeV/c, $S_L$ should not deviate more than a few percent from unity due to nucleon-nucleon correlations, and reach unity at higher $q$-values, independent of the nucleon-nucleon force chosen. Thus, a result of $S_L$ far from unity might indicate a possible modification of the nucleon electric properties in the nuclear medium at moderate distances (for example a change in the pion cloud charge distribution) while at very short distances the nucleon hard core might remain unmodified. While there are several theoretical approaches (for example, see Ref. [4] and references therein) on how to treat nucleons in nuclei the experimental situation is not ideal to help settle the important theoretical issues.

In the last twenty years a large experimental program has been carried out at Bates [5, 6, 7, 8, 9, 10, 11, 12], Saclay [13, 14, 15, 16, 17] and SLAC [18, 19] aimed at the extraction of $R_L$ and $R_T$ for a variety of nuclei. Overall consistency of the data set between different laboratories has been observed except for $^{40}$Ca between Bates [12] and Saclay [14, 15].

At Bates and Saclay, Rosenbluth separations were only performed up to $q$ of 550 MeV/$c$, because of the maximum beam energy limitations ($\sim$800 MeV/$c$), while at SLAC, only a measurement at $q$=1140 MeV/$c$ was performed due to the minimum beam energy available ($\sim$900 MeV/$c$). In this respect, Jefferson Lab offers a unique opportunity to overlap and extend the world data on $R_L$ and $R_T$ with a significantly improved precision.

In the case of medium-weight and heavy nuclei conclusions reached by different experiments ranged from a full saturation of the CSR to its violation by 30 %. As a result a spectrum of explanations has emerged ranging from questioning the validity of the experiments (i.e., experimental backgrounds and inadequate Coulomb corrections especially for heavy nuclei) to suggesting a picture of a "swollen nucleon" in the nuclear medium due to a partial deconfinement [20, 21, 22, 23].

A recent analysis by Jourdan [24, 25] which included data from all laboratories and uses Coulomb corrections through a Local Effective Momentum Approximation (LEMA) calculation by the Ohio group [26], concluded that the data are consistent with the saturation of the Coulomb Sum Rule, $S_L(q = 570\ \mathrm{MeV}/c) = 0.91 \pm 0.12$. The LEMA is supported by a full Distorted Wave Born Approximation (DWBA), however, it has been shown recently [27], by comparing quasi-elastic electron and positron scattering off $^{12}$C and $^{208}$Pb, that the Effective Momentum Approximation (EMA) can adequately describe quasi-elastic scattering, at variance with the LEMA calculations by the Ohio group [26].

We also point out that the error bar on $S_L$ is underestimated because the systematic error contributions resulting from the use of several laboratory data are poorly known. Furthermore, at the $q$ value chosen, extrapolations were necessary for $R_L$ at the excitation energies in the dip region, leading to a larger uncertainty in the evaluation of systematic errors.

A global reanalysis of the existing data was undertaken by Morgenstern and Meziani (M&M) using the EMA to correct for the Coulomb corrections and Rosenbluth separations were performed to extract $R_L$ and $R_T$ for medium weight and heavy nuclei. The quantitative difference of the experimental Coulomb sum results between Jourdan analysis and M&M analysis [28] is summarized in Table 1. Two sources of difference are identified; (a) the Coulomb corrections and (b)

Table 1: Comparison of the Coulomb Sum in $^{56}$Fe, obtained by Jourdan and from the M&M analysis at $q = 570\ \mathrm{MeV}/c$. (*) No SLAC data were used in this case.

| Analysis | Saclay Uncertainty | SLAC Uncertainty | Coulomb Correction | $S_L$ |
|---|---|---|---|---|
| Jourdan | total | statistical | No | 0.86±0.12 |
| | total | statistical | Yes | 0.91±0.12 |
| M&M | total | (*) | No | 0.72±0.23 |
| | total | (*) | Yes | 0.63±0.20 |
| | total | total | No | 0.82±0.12 |
| | total | total | Yes | 0.73±0.12 |

the use of the total error in the Saclay data but only the statistical error in the SLAC data by Jourdan. For (a), the Coulomb corrections used in [24, 25] following the prescription of [26], at variance with the experimental confirmation of the EMA [27], have the opposite sign; they increase $R_L$ instead of decreasing it. From Figs. 8 and 9 of Ref. [27] it is clear that these corrections reduce the magnitude of the large $\omega$ tail while in the case of [26] they enhance it: the Coulomb corrections of M&M reduce $S_L$ by 10% while Jourdan's increase it by 5%. The reduction of $R_L$ when using the EMA was already observed in the analysis of SLAC experiment NE9 [18]. For (b), more weight was given to the SLAC NE3 data by using only their statistical error in the Rosenbluth procedure leading to an artificial enhancement of $R_L$ by 4$\%$.

Figure 1 shows the results obtained for $S_L$ of $^{40}$Ca, $^{48}$Ca, $^{56}$Fe and $^{208}$Pb in this new analysis[28]. In order to evaluate $S_L$ the Simon [29] parametrization was used for the proton charge form factor, while for the neutron charge form factor the recent data by Herberg *et al.* [30] were taken into account. The results are compared to theoretical calculations for nuclear matter [31] (solid black curve) and $^4$He [32] (dashed curve); the results in these two cases as expected are very similar and exhibit only a few percent quenching beyond $q_{eff} \sim 500$ MeV/c. The experimental results are to be compared with the long-dashed curve which corresponds to the same calculations as the solid curve but integrated within the experimental limits of excitation energy $\omega$. A quenching of between 20$\%$ and 30$\%$ in medium weight nuclei persists.

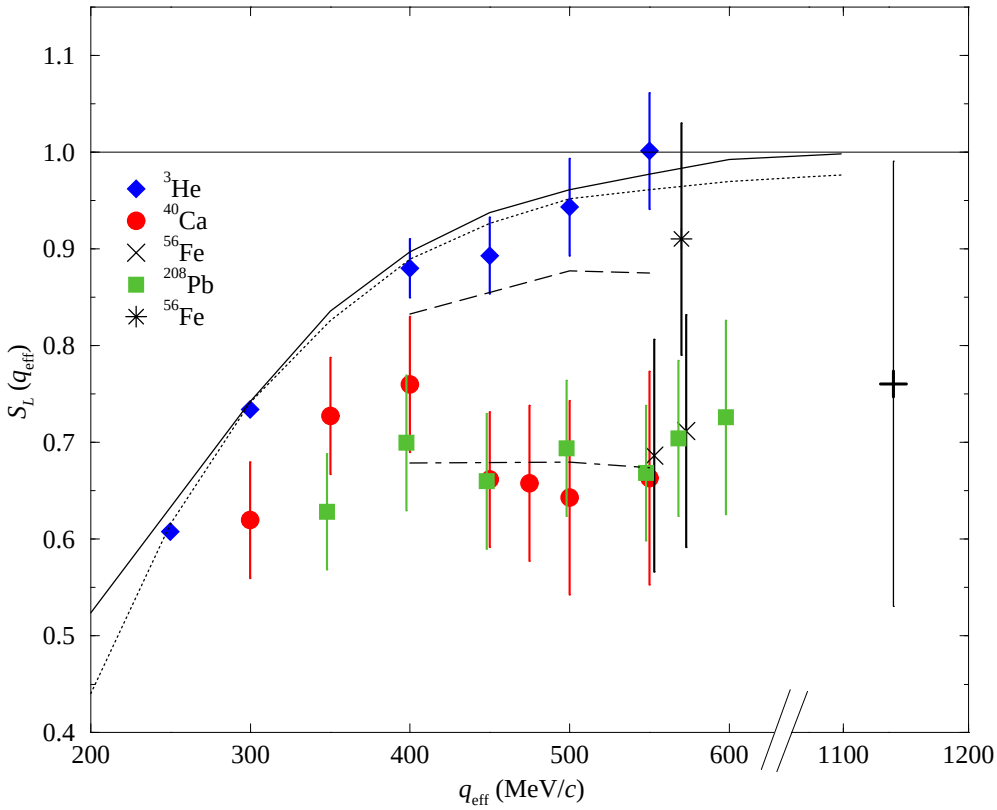


Figure 1: $S_L$ obtained in the EMA as a function of $q_{eff}$ using Saclay data combined with SLAC NE3 and Bates data. The $^{56}$Fe SLAC NE9 result [18] (right cross) and that of the Jourdan analysis (star) are also shown. For the curves see the text.

While the interpretation of the results is still open to debate it is our aim in this proposal to provide for a significantly improved experimental data in a momentum transfer region mainly unexplored. There is one result at $q$ = 1140 MeV/c from SLAC NE9 , but the experimental uncertainty leaves large room for constraining theoretical models of the Coulomb sum rule. Of course the momentum transfer range is chosen to overlap with previous measurements in order to settle the issue of the existence of quenching once and for all but investigating the $q$ evolution of $R_L$ in a totally unchartered territory is also of paramount importance.

At Jefferson Lab, we can make a measurement with improved precision compared to the existing data. We propose to measure the evolution of the Coulomb sum between $q = 550$ MeV/$c$ and $q = 1000$ MeV/$c$ in order to verify/refute its

quenching at moderate momentum transfer and to investigate its saturation at high momentum transfer. This measurement will be performed on several targets from $^4$He to $^{208}$Pb in order to address the issue of density dependence and Coulomb corrections. Whether the explanation of effects is from short range correlations or electromagnetic properties modifications, this new measurement will have a positive impact on our understanding of the behavior of nucleons in the nuclear medium.

## 2 Separation of $R_L$ and $R_T$

Under the assumption of one-photon exchange, the differential cross section of the inclusive electron scattering can be written as follows:

$$\frac{d^3\sigma}{d\Omega d\omega} = \sigma_{\rm M}\left[\frac{Q^4}{\mathbf{q}^4}R_L(|\mathbf{q}|,\omega)+\frac{Q^2}{2\mathbf{q}^2}\frac{R_T(|\mathbf{q}|,\omega)}{\varepsilon}\right]$$

where

$$\varepsilon(|\mathbf{q}|,\omega,\theta)=\left[1+\frac{2\mathbf{q}^2}{Q^2}\tan^2\frac{\theta}{2}\right]^{-1},$$

$Q^2=\mathbf{q}^2-\omega^2$ gives the four-momentum squared of the exchanged virtual photon, $\varepsilon$ is its polarization parameter, $\omega$ is the energy loss of the scattered electron, $\theta$ its laboratory scattering angle, $\sigma_{\rm M}$ is the Mott cross section, and $R(|\mathbf{q}|,\omega,\theta)$ is the total response function.

In order to extract $R_L$ and $R_T$, we need to measure the cross sections at a minimum of two different angles keeping $|\mathbf{q}|$ and $\omega$ constant. Let $\sigma_f$ and $\sigma_b$ be the cross sections measured at the forward ($f$) and backward ($b$) angles respectively. In the same way, let $\varepsilon_f$ and $\varepsilon_b$ be the two corresponding virtual photon polarizations. Then solving two simultaneous linear equations lead us to the following expressions for $R_L$ and $R_T$:

$$\begin{aligned} R_L &= \frac{|\mathbf{q}|^4}{Q^4\sigma_{\rm M}}\frac{1}{(\varepsilon_f-\varepsilon_b)}(\varepsilon_f\sigma_f-\varepsilon_b\sigma_b) \\ R_T &= \frac{|\mathbf{q}|^2}{Q^2\sigma_{\rm M}}\frac{2\varepsilon_f\varepsilon_b}{(\varepsilon_f-\varepsilon_b)}(\sigma_b-\sigma_f) \end{aligned}$$

The final goal of the measurement is to study the response functions at constant $|\mathbf{q}|$. However, keeping $|\mathbf{q}|$ constant is almost impractical since in Hall A, it

involves continuous change of beam and scattered electron energies. Instead, at constant angle but various, discrete values of the beam energy, we can cover as much space as possible in the $(\mathbf{q}, \omega)$ domain by changing continuously the energy of the scattered electrons. Then, by using an appropriate interpolation method we can deduce the cross section at specific values of $(\mathbf{q}, \omega)$. Once forward and backward cross sections at specfic values of $(\mathbf{q}, \omega)$ have been determined, we use the Rosenbluth separation to extract $R_L$ and $R_T$ for each $(\mathbf{q}, \omega)$.

# 3 Kinematics

In order to minimize the uncertainty in $R_L$, it is important to measure the cross section at the largest and smallest $\varepsilon$ possible (or the most forward and backward angle, respectively). For the most forward angle, we chose $15^\circ$ although the spectrometers in Hall A can be moved a little more forward with the presence of technicians. Our choice is close enough to the most forward angle without overhead time for special handling.

For the backward angle, we need to find a compromise with rapidly dropping counting rates and the lowest detectable energy by the spectrometers. We also find $120^\circ$ to be the largest angle practical given these constraints. This allows for the largest Rosenbluth lever arm within a single experiment compared to all previous experiments.

In order to perform a Rosenbluth separation, the minimum number of necessary angles is two. However, having additional angles enables us to check for any angle dependent systematic errors and the linearity of the Rosenbluth plot. We choose two more angles $60^\circ$ and $90^\circ$, which gives us four $\varepsilon$ approximately equally spaced.

To have as much coverage as possible in $(\mathbf{q}, \omega)$ to reduce systematic uncertainties in the interpolation procedure, we need beam energies ranging from 400 MeV to 4 GeV. For the most forward angle, the necessary beam energies range from 1.2 GeV to 4.0 GeV. For all the other angles, we need beam energies ranging from 0.4 GeV to 1.2 GeV. Taking data at various beam energies at four constant scattering angles has an added advantage of reducing systematic uncertainties in the radiative corrections procedure. Finally, the measurement at high $\omega$ requires spectrometer momentum settings down to $100\ \mathrm{MeV}/c$.

With this choice of kinematics, we can measure response functions from $|\mathbf{q}| = 550\mathrm{MeV}/c$ to 1000 $\mathrm{MeV}/c$. At each $|\mathbf{q}|$, the excitation energy range covers the quasi-elastic peak and part of $\Delta$-resonance where $R_L$ is expected to be small or

close to zero[33].

Figures 2 to 5 show the actual coverage in $Q^2$ and $\omega$ for each spectrometer momentum setting at the most forward and backward angles. In the figures, lines are drawn showing constant $|\mathbf{q}| = 550\ \mathrm{MeV}/c$ and $1000\ \mathrm{MeV}/c$ and $W = 940\ \mathrm{MeV}/c^2$ and $1232\ \mathrm{MeV}/c^2$. Table 5 lists all the kinematic settings.

# 4 Estimation of Accuracy of $R_L$ and $R_T$

We can estimate the uncertainty in the extracted response functions due to the relative statistical uncertainty $\Delta\sigma/\sigma$, the lever arm $\Delta\varepsilon$ and the ratio $\sigma_L/\sigma_T$. The uncertainty is expressed as:

$$\begin{aligned}
\frac{\Delta R_L}{R_L} &= \frac{\Delta\sigma}{\sigma}\frac{1}{\Delta\varepsilon}\sqrt{\left(\frac{1}{R}+\varepsilon_f\right)^2+\left(\frac{1}{R}+\varepsilon_b\right)^2} \\
\frac{\Delta R_T}{R_T} &= \frac{\Delta\sigma}{\sigma}\frac{R}{\Delta\varepsilon}\sqrt{\varepsilon_f^2\left(\frac{1}{R}+\varepsilon_b\right)^2+\varepsilon_b^2\left(\frac{1}{R}+\varepsilon_f\right)^2}
\end{aligned}$$

In this expression, $R = \sigma_L/\sigma_T$ is the ratio of longitudinal and transverse virtual photo-absorption cross sections. From these two expressions, we note that the uncertainty in the extracted response functions is inversely proportional to $\Delta\varepsilon$. Figure 6 shows the difference of the virtual photon polarization $\varepsilon$ between the forward and backward angle for a few values of $|\mathbf{q}|$. Typically, we can achieve $\Delta\varepsilon = \varepsilon_f - \varepsilon_b = 0.85$ compared to a typical $\Delta\varepsilon \simeq 0.5$ in the previous measurements. The increase in $\Delta\varepsilon$ achievable in Hall A of Jefferson Lab combined with low relative systematic uncertainties in the determination of beam energy, its position and scattering angle makes a crucial improvement in the uncertainties on the extraction of the response functions and therefore on the Coulomb Sum determination.

Using $R = \sigma_L/\sigma_T$ values for $^{56}$Fe from [14, 15, 18] and assuming statistical uncertainty of 1% for each 10 MeV excitation energy bin, the statistical uncertainty of $R_L$ at the quasi-elastic peak has been estimated for the two values of $|\mathrm{q}|$. Figures 7 and 8 shows the comparison of expected statistical uncertainties at Jefferson Lab with the existing data. We can achieve more data points with better statistical precision.

# 5 Experiment

We propose to measure cross sections over the whole quasi-elastic scattering and part of the $\Delta$ resonance region on $^4$He, $^{12}$C, $^{56}$Fe and $^{208}$Pb at four different angles and 16 incident beam energies as a function of $A$ and nuclear density.

## 5.1 Target

Our choice of targets ranging from $^4$He to $^{208}$Pb allows us to study any $A$ or density dependent effect one might observe. Furthermore, Coulomb corrections can be addressed by the same targets since we expect small Coulomb corrections for $^4$He and $^{12}$C, but rather significant corrections for $^{208}$Pb.

For $^4$He target, we plan to use Hall-A Cryo target which provides $^4$He gas at 15 atmospheres at 5.8K. The length of the target is 10 cm so the density is equal to 1.4 g/cm$^2$. Due to the short length of $^4$He target, we also need to do a measurement on a dummy cell to measure the contribution from the cell windows. For the nuclei other than $^4$He, solid targets of thickness 100 mg/cm$^2$ will be used. For $^{208}$Pb, two different target thicknesses will be used to check the radiative corrections.

## 5.2 Beam Current

The trigger rate for each spectrometer is limited to 2 kHz and this limits the used beam current. With the new helium cooled $^{56}$Fe and $^{208}$Pb target in Hall A, we can use up to 50 $\mu$A without damage due to heat produced by energy loss of the beam in the target. For the $^4$He gas target, we can use a much higher beam current, but to avoid too much change in target density at high beam current, we plan to use only 50 $\mu$A for maximum beam current. The beam will be rasterized to reduce localized heating and possible damage to the target.

## 5.3 Spectrometers

Since this experiment is not a coincidence measurement, the two spectrometers of Hall-A can do independent measurements at a given beam energy. We shall optimize the angle settings to minimize the overhead of momentum and angle changes.

# 6 Background Considerations

There are three major sources of contamination in the measured cross section: pions, electrons from $\gamma$ rays and scattering of electrons inside the spectrometer. The pion cross section increases as the energy transfer $\omega$ to the nucleus increases. However, using the Čerenkov and the Pb-glass detectors of the Hall A spectrometers, we have achieved typical pion rejection ratio of 5000.

The lowest scattered electron energy we will detect is 100 MeV at the backward angles. At this low energy spectrometer setting, the contribution of electrons from $(e^+, e^-)$ pairs created from $\gamma$ rays by the bremsstrahlung of the beam or by the decay of $\pi^0$ produced in the target needs to be subtracted from the electron yields. By reversing the polarity of the spectrometer with the detection system unchanged, we can measure the positron yields from this process and subtract an equal amount from the electron yields assuming charge symmetry of the process.

The scattering of the electrons inside the spectrometer, such as pole tip scattering usually generates uniform background on the focal plane. In particular, the measured momentum via reconstructed tracks in the wire chamber does not correspond to the actual momentum of the particle. This type of contamination could be important especially at the backward angles where the reaction cross sections are small.

We plan to study this type of background using the existing data from Hall A and our own Monte-Carlo simulation.

To eliminate this kind of contamination, it is most effective to use a customized collimator so that no particles accepted by the spectrometer will scatter on the matter inside of it. From the Monte-Carlo simulation, we can design and build a few different shapes for the collimator. To choose an optimal shape, we need additional beam time to measure the rates of the scattered electrons inside the spectrometer. Once the study is done, we can choose one of the customized collimators which will eliminate this type of background.

# 7 Systematic Errors

To estimate systematic errors, we start from the cross section expression:

$$\frac{d^3\sigma}{d\Omega d\omega} = \frac{N_{\rm detected}(1.0+\varepsilon_i)(1.0+{\rm DT})}{\left(\int \frac{\rho N_A}{A} dx\right)\left(\int \frac{I}{e} dt\right)\left(\int d\Omega d\omega\right)},$$

where

$$
\begin{aligned}
N_{\mathrm{detected}} &= \text{Number of events detected} \\
\varepsilon_i &= \text{Inefficiency of the detector system} \\
\mathrm{DT} &= \text{Dead Time} \\
\rho &= \text{Density of the target} \\
N_A &= \text{Avogadro Number}, 6.022 \times 10^{23} \\
A &= \text{Atomic number of the target} \\
I &= \text{Beam current} \\
e &= \text{Charge of the electron}, 1.602 \times 10^{-19}\mathrm{C}
\end{aligned}
$$

- The uncertainty on the detector inefficiencies is less than 0.3%.
- There are two kinds of dead time corrections: one from the electronics and the other from the computer. The electronics dead time is less than 1%. The computer dead time can be as big as 10% depending on the counting rate but is monitored continuously with scalers. The systematic error on this computer dead time is much smaller than 0.3%.
- For solid targets, the thickness of the target can be measured within 0.5%. With $^4$He gas target, in previous experiments, the thickness has been determined with an accuracy of $\sim$1%. To reduce the uncertainty on the target thickness for $^4$He target, we plan to study the fluctuation of the target density due to the beam heating and correct for it.
- The beam current is measured with several, independent method in Hall-A and an accuracy of 0.3% has been achieved.
- The acceptance of the spectrometer is determined using a Monte-Carlo simulation for each spectrometer. Currently available simulation model gives 1.0% of systematic error point-to-point within the acceptance for a point target. For an extended target like $^4$He, it will be about 1.5% using reduced acceptance cut. To minimize this uncertainty, some $^{12}$C elastic data will be taken for the acceptance calibration purposes for each beam energy and spectrometer angle setting.[1]

[1]The uncertainty on the overall normalization is about 3% but would affect the $R_L$ result only by the same amount (3%) since it changes cross sections at forward and backward angle by the same factor.

| Source | Solid Target | Gas Target |
|---|---|---|
| Beam Energy ($4 \times 10^{-4}$) | <0.3 | <0.3 |
| Momentum reconstruction | <0.3 | <0.3 |
| Detector Inefficiency | <0.3 | <0.3 |
| Dead Time Corrections | <0.3 | <0.3 |
| Interpolation | <0.3 | <0.3 |
| Beam Current | <0.3 | <0.3 |
| Scattering Angle (0.2 mrad) | 0.5 | 0.5 |
| Background | 0.5 | 0.5 |
| Target Density (relative) | 0.5 | 1.0 |
| Radiative Corrections | 1.0 | 1.0 |
| Acceptance (relative) | 1.0 | 1.5 |
| Total | 1.7 | 2.2 |

Table 2: Major contributions to the systematic uncertainty (in %).

In addition, there is another contribution from the radiative corrections which is discussed in the next section. From past experience, we expect 1% of systematic error from the radiative corrections.

Since we are doing a Rosenbluth separation of $R_L$ and $R_T$, the uncertainty on the spectrometer angle or beam energy contributes to the systematic uncertainties on both response functions and the Coulomb Sum.

- The uncertainty of the spectrometer angle (0.7 mrad for Hall A spectrometers) has effects of 1 to 1.5 % on $R_L$. We plan to reduce this uncertainty to 0.2 mrad by taking calibration data at each angle.

- The uncertainty of the beam energy ($2 \times 10^{-4}$) has effects of less than 0.3%

Finally, there is a systematic uncertainty from the interpolation of cross sections to constant $|\mathbf{q}|$ and we estimate it to be 0.5%. Table 2 summarizes all the major contributions to the systematic uncertainty.

By adding all the contributions in quadrature except that from the beam energy uncertainty, we can achieve a systematic error on the interpolated cross sections of 2.2% and 1.7% for $^4$He gas target and solid targets, respectively. This means that the final systematic uncertainty on $R_L$ will be 2.2 and 1.7 times the statistical uncertainty. Then the contribution from the scattering angle uncertainty (0.5%)

should be added in quadrature. The final estimate of systematic uncertainties are plotted on Figures 7, 8 and 9.

# 8 Radiative Corrections

After removing all the backgrounds described above, the resulting cross sections need to be corrected for radiative effects. We will use the Mo and Tsai procedure without any energy or angular peaking approximations. Since we have taken enough spectra at various incident energies, we should be able to do reliable radiative corrections and achieve a systematic error less than 1%. Two target thicknesses will be used for $^{208}$Pb to verify the external radiative corrections.

# 9 Coulomb Corrections for High $Z$ Nucleus

Among the chosen targets, we expect the Coulomb corrections to be negligible for $^{4}$He and $^{12}$C. However, for high $Z$ nucleus, such as $^{208}$Pb, they can be significant. In the literature, two methods for performing the Coulomb corrections have been used: one used by Jourdan[24, 25] in his recent analysis which applied Coulomb corrections through LEMA (tested to be consistent with a full DWBA calculation by the Ohio group.[26]), the other known as standard EMA[34] used recently to describe successfully $e^+$ and $e^-$ quasi-elastic scattering off $^{208}$Pb[27].

In the EMA, the energies of the incident and scattered electron $E$ and $E'$ are replaced by $E_{\rm eff} = E - V_C$ and $E'_{\rm eff} = E' - V_C$, where $V_C$ is the value of the effective Coulomb potential energy seen by the electron during the scattering process. The Rosenbluth formula can then be applied if we replace $Q^2$ and $\mathbf{q}^2$ by $Q^2_{\rm eff}$ and $\mathbf{q}^2_{\rm eff}$, respectively, while leaving the Mott cross section unchanged.[34] The values of $V_C$ can be taken from Table II of Ref. [27].

At this time, LEMA does not reproduce the recent $e^+/e^-$ quasi-elastic scattering data. However, the full DWBA calculation has not been checked against the same data and we expect this issue to be resolved in the near future.

To analyze our experiment, we will use whatever Coulomb correction method deemed to be correct and reliable.

# 10 Counting Rates and Required Time

To estimate the cross sections, we used the program by Lightbody and O'Connel. To evaluate the required time to do the measurement, we used a small solid angle of 4.4 msr for collimator solid angle of Hall-A spectrometer and $\pm$ 3.5% for the momentum acceptance. Beam current has been maintained under 50 $\mu$A. Also, the counting rate by the data acquisition system is limited to 2 kHz per spectrometer.

The number of counts per second is given by the following formula:

$$\text{event rate} = \frac{d^3\sigma}{d\Omega d\omega}\Delta\omega\Delta\Omega\frac{tN_A}{A}\frac{I}{e},$$

where

$t$ is the target thickness (we used 100 $mg/cm^2$),
$N_A = 6.022 \times 10^{23}$ is the Avogadro number,
$A$ is the mass number of the target nucleus,
$I$ is the beam current, and $e$ is the charge of the electron.

From these conditions, we have evaluated the necessary time to obtain statistical error of 1% per 10 MeV excitation energy bin. Table 4 shows estimated data acquisition time for each incident beam energy and spectrometer angle setting. Each line represents time required to take data on all four targets. Since we can use both spectrometers in Hall-A simultaneously to do measurements, the actual required time for data taking will be about 70% of the estimated time.[2]

All the overhead is summarized in Table 3. For the beam energy change, we assumed 1 shift for the change of number of passes and 2 shifts when it is necessary to fine-tune individual cavities. We have regrouped the beam energies as follows (all energies are in GeV).

$$(0.8, 1.6, 2.4, 3.2, 4.0), \quad (0.5, 1.0, 2.0), \quad (0.9, 3.6)$$
$$(0.7, 2.8), \quad (0.6, 1.2), \quad (1.1), \quad (0.4)$$

It takes one shift to change energies within the same group since we only need to change number of passes. However, it takes two shifts to change from one group

[2]The two spectrometers are not measuring the same configuration in general. At high energy and the most forward angle measurement, they can be at the same angle but at different momentum settings. For all the other energies, one spectrometer (A) will be at backward angle while the other (B) is at forward angle. In general, the forward angle measurements are short and spectrometer A can then move to a backward angle to minimize waste of time.

| Item | Time (Hour) |
|---|---|
| Beam Energy Change | $21 \times 8 = 168$ |
| Beam Energy Measurement | $16 \times 2 = 32$ |
| Beam Current Calibration | $4 \times 1 = 4$ |
| Spectrometer Acceptance Calibration Data | $28 \times 3/4 = 21$ |
| Spectrometer Change (Angle & Momentum) | $286 \times 0.5 \times 0.7 = 100.1$ |
| Target Change | $143 \times 5 \times 1/12 = 59.6$ |
| Set-up and Test | $3 \times 24 = 72$ |
| Total | 456.7 (= 19 days) |

Table 3: Estimation of the overhead

to another. So, we need 9 changes in number of passes and 6 changes of LINAC energies, requiring a total of 21 shifts.

There are two methods to do beam energy measurements: $e$p and Arc measurements. We assigned one hour for each method. Beam current calibration requires one hour for each beam energy.

We would like to take some $^{12}$C elastic data for spectrometer acceptance calibration for each beam energy and spectrometer angle. For this we need $1/2$ hour to change the spectrometer configuration and another 15 minutes to take data.

There is a total of 286 different settings for spectrometer angle and momemtum and each change of setting requires $1/2$ hour. Since we are using two spectrometers, we also expect that this overhead will be reduced by 30%.

A target change takes 5 minutes and there are 5 targets for each momentum setting ($^3$He, $^{12}$C, $^{56}$Fe and two different thicknesses for $^{206}$Pb).

Finally, we need 3 days in the beginning for set-up and testing.

By adding the time for data taking and overhead, we reach 29 days of beam time for this measurement.

As mentioned in Section 6 on the important background issue, we need to study the electrons scattered inside the spectrometer to design an optimal collimator which reduces to negligible level or eliminates the effect. For this study, we also ask for a separate beam time of three days before the main experiment.

# 11 Summary

We propose to make a precision measurement of $R_L$ and $R_T$ of quasi-elastic electron scattering in the momentum transfer range $0.55\ \mathrm{GeV}/c \leq |\mathbf{q}| \leq 1.0\ \mathrm{GeV}/c$. The experiment will measure inclusive electron scattering cross section at various kinematic conditions (beam and scattered electron energy and scattering angle) on four nuclei: $^{4}$He, $^{12}$C, $^{56}$Fe and $^{208}$Pb. Using $R_L$, we will evaluate the Coulomb Sum and study its evolution in the momentum range mentioned above. This new measurement will shed light on nucleon properties in the nuclear medium for various nuclear densities.

To do this measurement, we ask for 29 days of beam time and three additional days before the main experiment to study backgrounds from the electrons scattered inside the spectrometer.

# References


[1] M. Birse, J. Phys. **G20**, (1994) 1537.

[2] K.W. McVoy and L. Van Hove, Phys. Rev. **125**, (1962) 1034.

[3] T. de Forest, Jr., Nucl. Phys. **A414** (1984) 347.

[4] M. R. Frank, B. K. Jennings and G. A. Miller, Phys. Rev. C **54**, 920 (1996).

[5] R. Altemus *et al.,* Phys. Rev. Lett. **44**, 965 (1980).

[6] M. Deady *et al.,* Phys. Rev. C **28**, 631 (1983).

[7] A. Hotta *et al.,* Phys. Rev. C **30**, 87 (1984).

[8] M. Deady *et al.,* Phys. Rev. C **33**, 1897 (1986).

[9] C.C. Blatchley *et al.,* Phys. Rev. C **34**, 1243 (1986).

[10] S.A. Dytman *et al.,* Phys. Rev. C **38**, 800 (1988).

[11] T.C. Yates *et al.,* Phys. Lett. **312B**, 382 (1993).

[12] C. Williamson *et al.,* Phys. Rev. C **56**, 3152 (1997).

[13] P. Barreau *et al.,* Nucl. Phys. **A402**, 515 (1983).

[14] Z.-E. Meziani *et al.,* Phys. Rev. Lett. **52**, 2130 (1984).

[15] Z.-E. Meziani *et al.,* Phys. Rev. Lett. **54**, 1233 (1985).

[16] C. Marchand *et al.,* Phys. Lett. **153B**, 29 (1985).

[17] A. Zghiche *et al.,* Nucl. Phys. **A572**, 513 (1994).

[18] J. P. Chen *et al.,* Phys. Rev. Lett. **66**, 1283 (1991).

[19] Z.-E. Meziani *et al.,* Phys. Rev. Lett. **69**, 41 (1992).

[20] J. V. Noble, Phys. Rev. Lett. **46**, 412 (1981).

[21] L. S. Celenza *et al.,* Phys. Rev. Lett. **53**, 891 (1984).

[22] P. J. Mulders, Nucl. Phys. A **459**, 525 (1986).

[23] G.E. Brown and M. Rho, Phys. Lett. **222B**, 324 (1989).

[24] J. Jourdan, Phys. Lett. **353B**, 189 (1995).

[25] J. Jourdan, Nucl. Phys. **A603**, 117 (1996).

[26] D. Onley, Y. Yin and L. E. Wright, Phys. Rev. C **45**, 1333 (1992); K. S. Kim, L.E. Wright, Y. Yin and D. W. Kosik, Phys. Rev. C **54**, 2515 (1996).

[27] P. Gueye *et al.*, Phys. Rev. C **60**, 044308 (1999).

[28] J. Morgenstern and Z.-E. Meziani, submitted to Phys. Rev. Lett. and private communication.

[29] G.G. Simon *et al.*, Nucl. Phys. A **333**, 381 (1980).

[30] C. Herberg *et al.*, Eur. Phys. **A5**, 131 (1999).

[31] A. Fabrocini and S. Fantoni, Nucl. Phys. A **503**, 375 (1989).

[32] R. Schiavilla *et al.*, Nucl. Phys. A **499**, 301 (1989).

[33] D. T. Baran *et al.*, Phys. Rev. Lett. **61**, 400 (1988).

[34] R. Rosenfelder, Ann. Phys., **128**, (1980).

| $E_{\rm beam}$ | $\theta$ | No. of $P_{\rm ref}$ | Time (Hour) | Sub-Total (Hour) |
|---|---|---|---|---|
| 400.0 | 90.0° | 17 | 11.3 | |
| | 120.0° | 16 | 10.9 | 22.3 |
| 500.0 | 90.0° | 20 | 13.9 | |
| | 120.0° | 18 | 16.1 | 30.0 |
| 600.0 | 60.0° | 16 | 10.7 | |
| | 90.0° | 17 | 15.6 | |
| | 120.0° | 18 | 22.7 | 48.9 |
| 700.0 | 60.0° | 13 | 8.8 | |
| | 90.0° | 14 | 20.6 | |
| | 120.0° | 15 | 28.2 | 57.6 |
| 800.0 | 60.0° | 11 | 8.5 | |
| | 90.0° | 13 | 23.1 | |
| | 120.0° | 13 | 22.0 | 53.7 |
| 900.0 | 60.0° | 10 | 10.7 | |
| | 90.0° | 12 | 24.3 | |
| | 120.0° | 6 | 13.8 | 48.8 |
| 1000.0 | 60.0° | 9 | 15.3 | |
| | 90.0° | 6 | 11.4 | 26.8 |
| 1100.0 | 60.0° | 9 | 18.4 | 18.4 |
| 1200.0 | 15.0° | 6 | 4.0 | |
| | 60.0° | 8 | 20.2 | 24.2 |
| 1600.0 | 15.0° | 4 | 2.7 | 2.7 |
| 2000.0 | 15.0° | 3 | 2.0 | 2.0 |
| 2400.0 | 15.0° | 3 | 2.0 | 2.0 |
| 2800.0 | 15.0° | 3 | 2.0 | 2.0 |
| 3200.0 | 15.0° | 3 | 2.2 | 2.2 |
| 3600.0 | 15.0° | 2 | 1.8 | 1.8 |
| 4000.0 | 15.0° | 1 | 2.1 | 2.1 |
| Total Time (hours) | | | | 345.2 |
| With 2 Spectrometers | | | | 241.6 |

Table 4: Estimation of the required time at each beam energy

| $E_{\text{beam}}$ (MeV) | $\theta$ | $P_{\text{ref}}$ $(\text{MeV}/c)$ | $Q^2$ $(\text{GeV}^2)$ | $\omega$ (MeV) | $W$ $(\text{GeV}/c^2)$ |
|---|---|---|---|---|---|
| 400.0 | 90.0° | 103.895 | 0.0831 | 296.11 | 1.1650 |
| 400.0 | 90.0° | 111.431 | 0.0891 | 288.57 | 1.1563 |
| 400.0 | 90.0° | 119.514 | 0.0956 | 280.49 | 1.1469 |
| 400.0 | 90.0° | 128.184 | 0.1025 | 271.82 | 1.1367 |
| 400.0 | 90.0° | 137.482 | 0.1100 | 262.52 | 1.1257 |
| 400.0 | 90.0° | 147.455 | 0.1180 | 252.54 | 1.1137 |
| 400.0 | 90.0° | 158.151 | 0.1265 | 241.85 | 1.1008 |
| 400.0 | 90.0° | 169.623 | 0.1357 | 230.38 | 1.0867 |
| 400.0 | 90.0° | 181.927 | 0.1455 | 218.07 | 1.0715 |
| 400.0 | 90.0° | 195.124 | 0.1561 | 204.88 | 1.0548 |
| 400.0 | 90.0° | 209.278 | 0.1674 | 190.72 | 1.0367 |
| 400.0 | 90.0° | 224.459 | 0.1796 | 175.54 | 1.0169 |
| 400.0 | 90.0° | 240.741 | 0.1926 | 159.26 | 0.9952 |
| 400.0 | 90.0° | 258.204 | 0.2066 | 141.80 | 0.9714 |
| 400.0 | 90.0° | 276.934 | 0.2215 | 123.07 | 0.9452 |
| 400.0 | 90.0° | 297.023 | 0.2376 | 102.98 | 0.9163 |
| 400.0 | 90.0° | 318.568 | 0.2549 | 81.43 | 0.8842 |
| 400.0 | 120.0° | 102.432 | 0.1229 | 297.57 | 1.1490 |
| 400.0 | 120.0° | 109.863 | 0.1318 | 290.14 | 1.1390 |
| 400.0 | 120.0° | 117.832 | 0.1414 | 282.17 | 1.1281 |
| 400.0 | 120.0° | 126.379 | 0.1517 | 273.62 | 1.1164 |
| 400.0 | 120.0° | 135.547 | 0.1627 | 264.45 | 1.1037 |
| 400.0 | 120.0° | 145.379 | 0.1745 | 254.62 | 1.0899 |
| 400.0 | 120.0° | 155.925 | 0.1871 | 244.07 | 1.0749 |
| 400.0 | 120.0° | 167.235 | 0.2007 | 232.76 | 1.0585 |
| 400.0 | 120.0° | 179.366 | 0.2152 | 220.63 | 1.0407 |
| 400.0 | 120.0° | 192.377 | 0.2309 | 207.62 | 1.0213 |
| 400.0 | 120.0° | 206.332 | 0.2476 | 193.67 | 1.0000 |
| 400.0 | 120.0° | 221.299 | 0.2656 | 178.70 | 0.9767 |
| 400.0 | 120.0° | 237.352 | 0.2848 | 162.65 | 0.9511 |
| 400.0 | 120.0° | 254.569 | 0.3055 | 145.43 | 0.9228 |
| 400.0 | 120.0° | 273.036 | 0.3276 | 126.96 | 0.8914 |

Table 5: Table of Kinematics

| $E_{\mathrm{beam}}$ (MeV) | $\theta$ | $P_{\mathrm{ref}}$ $(\mathrm{MeV}/c)$ | $Q^2$ $(\mathrm{GeV}^2)$ | $\omega$ (MeV) | $W$ $(\mathrm{GeV}/c^2)$ |
|---|---|---|---|---|---|
| 400.0 | 120.0° | 292.841 | 0.3514 | 107.16 | 0.8565 |
| 500.0 | 90.0° | 100.831 | 0.1008 | 399.17 | 1.2382 |
| 500.0 | 90.0° | 108.145 | 0.1081 | 391.86 | 1.2297 |
| 500.0 | 90.0° | 115.990 | 0.1160 | 384.01 | 1.2205 |
| 500.0 | 90.0° | 124.404 | 0.1244 | 375.60 | 1.2105 |
| 500.0 | 90.0° | 133.428 | 0.1334 | 366.57 | 1.1997 |
| 500.0 | 90.0° | 143.107 | 0.1431 | 356.89 | 1.1880 |
| 500.0 | 90.0° | 153.488 | 0.1535 | 346.51 | 1.1754 |
| 500.0 | 90.0° | 164.621 | 0.1646 | 335.38 | 1.1617 |
| 500.0 | 90.0° | 176.563 | 0.1766 | 323.44 | 1.1468 |
| 500.0 | 90.0° | 189.370 | 0.1894 | 310.63 | 1.1306 |
| 500.0 | 90.0° | 203.107 | 0.2031 | 296.89 | 1.1129 |
| 500.0 | 90.0° | 217.840 | 0.2178 | 282.16 | 1.0937 |
| 500.0 | 90.0° | 233.642 | 0.2336 | 266.36 | 1.0727 |
| 500.0 | 90.0° | 250.590 | 0.2506 | 249.41 | 1.0497 |
| 500.0 | 90.0° | 268.768 | 0.2688 | 231.23 | 1.0245 |
| 500.0 | 90.0° | 288.264 | 0.2883 | 211.74 | 0.9967 |
| 500.0 | 90.0° | 309.174 | 0.3092 | 190.83 | 0.9660 |
| 500.0 | 90.0° | 331.602 | 0.3316 | 168.40 | 0.9320 |
| 500.0 | 90.0° | 355.655 | 0.3557 | 144.35 | 0.8940 |
| 500.0 | 90.0° | 381.454 | 0.3815 | 118.55 | 0.8515 |
| 500.0 | 120.0° | 104.950 | 0.1574 | 395.05 | 1.2120 |
| 500.0 | 120.0° | 112.563 | 0.1688 | 387.44 | 1.2013 |
| 500.0 | 120.0° | 120.728 | 0.1811 | 379.27 | 1.1898 |
| 500.0 | 120.0° | 129.486 | 0.1942 | 370.51 | 1.1773 |
| 500.0 | 120.0° | 138.878 | 0.2083 | 361.12 | 1.1637 |
| 500.0 | 120.0° | 148.952 | 0.2234 | 351.05 | 1.1490 |
| 500.0 | 120.0° | 159.757 | 0.2396 | 340.24 | 1.1330 |
| 500.0 | 120.0° | 171.346 | 0.2570 | 328.65 | 1.1155 |
| 500.0 | 120.0° | 183.775 | 0.2757 | 316.23 | 1.0966 |
| 500.0 | 120.0° | 197.106 | 0.2957 | 302.89 | 1.0758 |
| 500.0 | 120.0° | 211.404 | 0.3171 | 288.60 | 1.0531 |

Table 6: Table of Kinematics (Continued)

| $E_{\mathrm{beam}}$ (MeV) | $\theta$ | $P_{\mathrm{ref}}$ $(\mathrm{MeV}/c)$ | $Q^2$ $(\mathrm{GeV}^2)$ | $\omega$ (MeV) | $W$ $(\mathrm{GeV}/c^2)$ |
|---|---|---|---|---|---|
| 500.0 | 120.0° | 226.739 | 0.3401 | 273.26 | 1.0282 |
| 500.0 | 120.0° | 243.186 | 0.3648 | 256.81 | 1.0008 |
| 500.0 | 120.0° | 260.826 | 0.3912 | 239.17 | 0.9706 |
| 500.0 | 120.0° | 279.747 | 0.4196 | 220.25 | 0.9370 |
| 500.0 | 120.0° | 300.039 | 0.4501 | 199.96 | 0.8997 |
| 500.0 | 120.0° | 321.803 | 0.4827 | 178.20 | 0.8578 |
| 500.0 | 120.0° | 345.147 | 0.5177 | 154.85 | 0.8106 |
| 600.0 | 60.0° | 174.826 | 0.1049 | 425.17 | 1.2562 |
| 600.0 | 60.0° | 187.508 | 0.1125 | 412.49 | 1.2436 |
| 600.0 | 60.0° | 201.110 | 0.1207 | 398.89 | 1.2300 |
| 600.0 | 60.0° | 215.698 | 0.1294 | 384.30 | 1.2152 |
| 600.0 | 60.0° | 231.344 | 0.1388 | 368.66 | 1.1991 |
| 600.0 | 60.0° | 248.126 | 0.1489 | 351.87 | 1.1816 |
| 600.0 | 60.0° | 266.125 | 0.1597 | 333.87 | 1.1626 |
| 600.0 | 60.0° | 285.429 | 0.1713 | 314.57 | 1.1418 |
| 600.0 | 60.0° | 306.134 | 0.1837 | 293.87 | 1.1191 |
| 600.0 | 60.0° | 328.340 | 0.1970 | 271.66 | 1.0942 |
| 600.0 | 60.0° | 352.158 | 0.2113 | 247.84 | 1.0669 |
| 600.0 | 60.0° | 377.703 | 0.2266 | 222.30 | 1.0368 |
| 600.0 | 60.0° | 405.101 | 0.2431 | 194.90 | 1.0035 |
| 600.0 | 60.0° | 434.486 | 0.2607 | 165.51 | 0.9665 |
| 600.0 | 60.0° | 466.004 | 0.2796 | 134.00 | 0.9252 |
| 600.0 | 60.0° | 499.807 | 0.2999 | 100.19 | 0.8787 |
| 600.0 | 90.0° | 143.257 | 0.1719 | 456.74 | 1.2531 |
| 600.0 | 90.0° | 153.648 | 0.1844 | 446.35 | 1.2403 |
| 600.0 | 90.0° | 164.794 | 0.1978 | 435.21 | 1.2264 |
| 600.0 | 90.0° | 176.748 | 0.2121 | 423.25 | 1.2113 |
| 600.0 | 90.0° | 189.569 | 0.2275 | 410.43 | 1.1949 |
| 600.0 | 90.0° | 203.320 | 0.2440 | 396.68 | 1.1770 |
| 600.0 | 90.0° | 218.069 | 0.2617 | 381.93 | 1.1576 |
| 600.0 | 90.0° | 233.887 | 0.2807 | 366.11 | 1.1363 |
| 600.0 | 90.0° | 250.853 | 0.3010 | 349.15 | 1.1131 |

Table 7: Table of Kinematics (Continued)

| $E_{\text{beam}}$ (MeV) | $\theta$ | $P_{\text{ref}}$ $(\text{MeV}/c)$ | $Q^2$ $(\text{GeV}^2)$ | $\omega$ (MeV) | $W$ $(\text{GeV}/c^2)$ |
|---|---|---|---|---|---|
| 600.0 | 90.0° | 269.050 | 0.3229 | 330.95 | 1.0876 |
| 600.0 | 90.0° | 288.566 | 0.3463 | 311.43 | 1.0596 |
| 600.0 | 90.0° | 309.499 | 0.3714 | 290.50 | 1.0288 |
| 600.0 | 90.0° | 331.949 | 0.3983 | 268.05 | 0.9946 |
| 600.0 | 90.0° | 356.028 | 0.4272 | 243.97 | 0.9566 |
| 600.0 | 90.0° | 381.854 | 0.4582 | 218.15 | 0.9141 |
| 600.0 | 90.0° | 409.553 | 0.4915 | 190.45 | 0.8661 |
| 600.0 | 90.0° | 439.262 | 0.5271 | 160.74 | 0.8116 |
| 600.0 | 120.0° | 119.136 | 0.2144 | 480.86 | 1.2543 |
| 600.0 | 120.0° | 127.778 | 0.2300 | 472.22 | 1.2415 |
| 600.0 | 120.0° | 137.047 | 0.2467 | 462.95 | 1.2277 |
| 600.0 | 120.0° | 146.988 | 0.2646 | 453.01 | 1.2127 |
| 600.0 | 120.0° | 157.651 | 0.2838 | 442.35 | 1.1964 |
| 600.0 | 120.0° | 169.086 | 0.3044 | 430.91 | 1.1787 |
| 600.0 | 120.0° | 181.352 | 0.3264 | 418.65 | 1.1594 |
| 600.0 | 120.0° | 194.507 | 0.3501 | 405.49 | 1.1383 |
| 600.0 | 120.0° | 208.616 | 0.3755 | 391.38 | 1.1153 |
| 600.0 | 120.0° | 223.749 | 0.4027 | 376.25 | 1.0900 |
| 600.0 | 120.0° | 239.979 | 0.4320 | 360.02 | 1.0623 |
| 600.0 | 120.0° | 257.387 | 0.4633 | 342.61 | 1.0317 |
| 600.0 | 120.0° | 276.058 | 0.4969 | 323.94 | 0.9979 |
| 600.0 | 120.0° | 296.083 | 0.5329 | 303.92 | 0.9602 |
| 600.0 | 120.0° | 317.560 | 0.5716 | 282.44 | 0.9181 |
| 600.0 | 120.0° | 340.596 | 0.6131 | 259.40 | 0.8708 |
| 600.0 | 120.0° | 365.302 | 0.6575 | 234.70 | 0.8169 |
| 600.0 | 120.0° | 391.801 | 0.7052 | 208.20 | 0.7548 |
| 700.0 | 60.0° | 245.996 | 0.1722 | 454.00 | 1.2510 |
| 700.0 | 60.0° | 263.841 | 0.1847 | 436.16 | 1.2324 |
| 700.0 | 60.0° | 282.979 | 0.1981 | 417.02 | 1.2122 |
| 700.0 | 60.0° | 303.506 | 0.2125 | 396.49 | 1.1902 |
| 700.0 | 60.0° | 325.522 | 0.2279 | 374.48 | 1.1661 |
| 700.0 | 60.0° | 349.135 | 0.2444 | 350.87 | 1.1397 |

Table 8: Table of Kinematics (Continued)

| $E_{\mathrm{beam}}$ (MeV) | $\theta$ | $P_{\mathrm{ref}}$ $(\mathrm{MeV}/c)$ | $Q^2$ $(\mathrm{GeV}^2)$ | $\omega$ (MeV) | $W$ $(\mathrm{GeV}/c^2)$ |
|---|---|---|---|---|---|
| 700.0 | 60.0° | 374.461 | 0.2621 | 325.54 | 1.1106 |
| 700.0 | 60.0° | 401.624 | 0.2811 | 298.38 | 1.0786 |
| 700.0 | 60.0° | 430.758 | 0.3015 | 269.24 | 1.0432 |
| 700.0 | 60.0° | 462.004 | 0.3234 | 238.00 | 1.0038 |
| 700.0 | 60.0° | 495.518 | 0.3469 | 204.48 | 0.9598 |
| 700.0 | 60.0° | 531.462 | 0.3720 | 168.54 | 0.9102 |
| 700.0 | 60.0° | 570.014 | 0.3990 | 129.99 | 0.8538 |
| 700.0 | 90.0° | 198.203 | 0.2775 | 501.80 | 1.2448 |
| 700.0 | 90.0° | 212.580 | 0.2976 | 487.42 | 1.2257 |
| 700.0 | 90.0° | 228.000 | 0.3192 | 472.00 | 1.2049 |
| 700.0 | 90.0° | 244.539 | 0.3424 | 455.46 | 1.1822 |
| 700.0 | 90.0° | 262.278 | 0.3672 | 437.72 | 1.1573 |
| 700.0 | 90.0° | 281.303 | 0.3938 | 418.70 | 1.1300 |
| 700.0 | 90.0° | 301.709 | 0.4224 | 398.29 | 1.1000 |
| 700.0 | 90.0° | 323.594 | 0.4530 | 376.41 | 1.0669 |
| 700.0 | 90.0° | 347.067 | 0.4859 | 352.93 | 1.0302 |
| 700.0 | 90.0° | 372.243 | 0.5211 | 327.76 | 0.9893 |
| 700.0 | 90.0° | 399.245 | 0.5589 | 300.75 | 0.9434 |
| 700.0 | 90.0° | 428.206 | 0.5995 | 271.79 | 0.8917 |
| 700.0 | 90.0° | 459.268 | 0.6430 | 240.73 | 0.8326 |
| 700.0 | 90.0° | 492.582 | 0.6896 | 207.42 | 0.7642 |
| 700.0 | 120.0° | 162.697 | 0.3417 | 537.30 | 1.2458 |
| 700.0 | 120.0° | 174.499 | 0.3664 | 525.50 | 1.2268 |
| 700.0 | 120.0° | 187.157 | 0.3930 | 512.84 | 1.2061 |
| 700.0 | 120.0° | 200.733 | 0.4215 | 499.27 | 1.1835 |
| 700.0 | 120.0° | 215.294 | 0.4521 | 484.71 | 1.1588 |
| 700.0 | 120.0° | 230.911 | 0.4849 | 469.09 | 1.1316 |
| 700.0 | 120.0° | 247.661 | 0.5201 | 452.34 | 1.1018 |
| 700.0 | 120.0° | 265.626 | 0.5578 | 434.37 | 1.0688 |
| 700.0 | 120.0° | 284.894 | 0.5983 | 415.11 | 1.0323 |
| 700.0 | 120.0° | 305.560 | 0.6417 | 394.44 | 0.9917 |
| 700.0 | 120.0° | 327.725 | 0.6882 | 372.27 | 0.9462 |

Table 9: Table of Kinematics (Continued)

| $E_{\mathrm{beam}}$ (MeV) | $\theta$ | $P_{\mathrm{ref}}$ $(\mathrm{MeV}/c)$ | $Q^2$ $(\mathrm{GeV}^2)$ | $\omega$ (MeV) | $W$ $(\mathrm{GeV}/c^2)$ |
|---|---|---|---|---|---|
| 700.0 | 120.0° | 351.498 | 0.7381 | 348.50 | 0.8948 |
| 700.0 | 120.0° | 376.995 | 0.7917 | 323.00 | 0.8362 |
| 700.0 | 120.0° | 404.342 | 0.8491 | 295.66 | 0.7683 |
| 700.0 | 120.0° | 433.672 | 0.9107 | 266.33 | 0.6882 |
| 800.0 | 60.0° | 316.302 | 0.2530 | 483.70 | 1.2409 |
| 800.0 | 60.0° | 339.246 | 0.2714 | 460.75 | 1.2159 |
| 800.0 | 60.0° | 363.855 | 0.2911 | 436.14 | 1.1885 |
| 800.0 | 60.0° | 390.248 | 0.3122 | 409.75 | 1.1583 |
| 800.0 | 60.0° | 418.557 | 0.3348 | 381.44 | 1.1251 |
| 800.0 | 60.0° | 448.918 | 0.3591 | 351.08 | 1.0883 |
| 800.0 | 60.0° | 481.482 | 0.3852 | 318.52 | 1.0475 |
| 800.0 | 60.0° | 516.408 | 0.4131 | 283.59 | 1.0018 |
| 800.0 | 60.0° | 553.868 | 0.4431 | 246.13 | 0.9504 |
| 800.0 | 60.0° | 594.045 | 0.4752 | 205.96 | 0.8919 |
| 800.0 | 60.0° | 637.136 | 0.5097 | 162.86 | 0.8247 |
| 800.0 | 90.0° | 233.872 | 0.3742 | 566.13 | 1.2545 |
| 800.0 | 90.0° | 250.836 | 0.4013 | 549.16 | 1.2307 |
| 800.0 | 90.0° | 269.032 | 0.4305 | 530.97 | 1.2047 |
| 800.0 | 90.0° | 288.547 | 0.4617 | 511.45 | 1.1762 |
| 800.0 | 90.0° | 309.478 | 0.4952 | 490.52 | 1.1448 |
| 800.0 | 90.0° | 331.927 | 0.5311 | 468.07 | 1.1102 |
| 800.0 | 90.0° | 356.005 | 0.5696 | 444.00 | 1.0718 |
| 800.0 | 90.0° | 381.829 | 0.6109 | 418.17 | 1.0290 |
| 800.0 | 90.0° | 409.526 | 0.6552 | 390.47 | 0.9810 |
| 800.0 | 90.0° | 439.233 | 0.7028 | 360.77 | 0.9269 |
| 800.0 | 90.0° | 471.094 | 0.7538 | 328.91 | 0.8650 |
| 800.0 | 90.0° | 505.267 | 0.8084 | 294.73 | 0.7933 |
| 800.0 | 90.0° | 541.919 | 0.8671 | 258.08 | 0.7083 |
| 800.0 | 120.0° | 189.704 | 0.4553 | 610.30 | 1.2553 |
| 800.0 | 120.0° | 203.465 | 0.4883 | 596.53 | 1.2316 |
| 800.0 | 120.0° | 218.224 | 0.5237 | 581.78 | 1.2057 |
| 800.0 | 120.0° | 234.053 | 0.5617 | 565.95 | 1.1772 |

Table 10: Table of Kinematics (Continued)

| $E_{\text{beam}}$ (MeV) | $\theta$ | $P_{\text{ref}}$ $(\text{MeV}/c)$ | $Q^2$ $(\text{GeV}^2)$ | $\omega$ (MeV) | $W$ $(\text{GeV}/c^2)$ |
|---|---|---|---|---|---|
| 800.0 | 120.0° | 251.031 | 0.6025 | 548.97 | 1.1459 |
| 800.0 | 120.0° | 269.241 | 0.6462 | 530.76 | 1.1114 |
| 800.0 | 120.0° | 288.771 | 0.6931 | 511.23 | 1.0732 |
| 800.0 | 120.0° | 309.718 | 0.7433 | 490.28 | 1.0305 |
| 800.0 | 120.0° | 332.185 | 0.7972 | 467.81 | 0.9828 |
| 800.0 | 120.0° | 356.281 | 0.8551 | 443.72 | 0.9288 |
| 800.0 | 120.0° | 382.126 | 0.9171 | 417.87 | 0.8672 |
| 800.0 | 120.0° | 409.845 | 0.9836 | 390.15 | 0.7959 |
| 800.0 | 120.0° | 439.574 | 1.0550 | 360.43 | 0.7115 |
| 900.0 | 60.0° | 373.450 | 0.3361 | 526.55 | 1.2399 |
| 900.0 | 60.0° | 400.539 | 0.3605 | 499.46 | 1.2092 |
| 900.0 | 60.0° | 429.594 | 0.3866 | 470.41 | 1.1753 |
| 900.0 | 60.0° | 460.756 | 0.4147 | 439.24 | 1.1378 |
| 900.0 | 60.0° | 494.179 | 0.4448 | 405.82 | 1.0963 |
| 900.0 | 60.0° | 530.026 | 0.4770 | 369.97 | 1.0498 |
| 900.0 | 60.0° | 568.474 | 0.5116 | 331.53 | 0.9976 |
| 900.0 | 60.0° | 609.710 | 0.5487 | 290.29 | 0.9384 |
| 900.0 | 60.0° | 653.938 | 0.5885 | 246.06 | 0.8704 |
| 900.0 | 60.0° | 701.374 | 0.6312 | 198.63 | 0.7911 |
| 900.0 | 90.0° | 272.028 | 0.4897 | 627.97 | 1.2548 |
| 900.0 | 90.0° | 291.760 | 0.5252 | 608.24 | 1.2255 |
| 900.0 | 90.0° | 312.924 | 0.5633 | 587.08 | 1.1933 |
| 900.0 | 90.0° | 335.623 | 0.6041 | 564.38 | 1.1578 |
| 900.0 | 90.0° | 359.969 | 0.6479 | 540.03 | 1.1184 |
| 900.0 | 90.0° | 386.081 | 0.6949 | 513.92 | 1.0746 |
| 900.0 | 90.0° | 414.087 | 0.7454 | 485.91 | 1.0256 |
| 900.0 | 90.0° | 444.124 | 0.7994 | 455.88 | 0.9702 |
| 900.0 | 90.0° | 476.340 | 0.8574 | 423.66 | 0.9070 |
| 900.0 | 90.0° | 510.893 | 0.9196 | 389.11 | 0.8340 |
| 900.0 | 90.0° | 547.953 | 0.9863 | 352.05 | 0.7478 |
| 900.0 | 90.0° | 587.701 | 1.0579 | 312.30 | 0.6425 |
| 900.0 | 120.0° | 218.256 | 0.5893 | 681.74 | 1.2554 |

Table 11: Table of Kinematics (Continued)

| $E_{\mathrm{beam}}$ (MeV) | $\theta$ | $P_{\mathrm{ref}}$ $(\mathrm{MeV}/c)$ | $Q^2$ $(\mathrm{GeV}^2)$ | $\omega$ (MeV) | $W$ $(\mathrm{GeV}/c^2)$ |
|---|---|---|---|---|---|
| 900.0 | 120.0° | 234.088 | 0.6320 | 665.91 | 1.2262 |
| 900.0 | 120.0° | 251.069 | 0.6779 | 648.93 | 1.1940 |
| 900.0 | 120.0° | 269.281 | 0.7271 | 630.72 | 1.1586 |
| 900.0 | 120.0° | 288.815 | 0.7798 | 611.18 | 1.1193 |
| 900.0 | 120.0° | 309.765 | 0.8364 | 590.24 | 1.0756 |
| 1000.0 | 60.0° | 435.681 | 0.4357 | 564.32 | 1.2283 |
| 1000.0 | 60.0° | 467.284 | 0.4673 | 532.72 | 1.1907 |
| 1000.0 | 60.0° | 501.181 | 0.5012 | 498.82 | 1.1490 |
| 1000.0 | 60.0° | 537.536 | 0.5375 | 462.46 | 1.1025 |
| 1000.0 | 60.0° | 576.528 | 0.5765 | 423.47 | 1.0503 |
| 1000.0 | 60.0° | 618.349 | 0.6183 | 381.65 | 0.9913 |
| 1000.0 | 60.0° | 663.203 | 0.6632 | 336.80 | 0.9239 |
| 1000.0 | 60.0° | 711.311 | 0.7113 | 288.69 | 0.8456 |
| 1000.0 | 60.0° | 762.909 | 0.7629 | 237.09 | 0.7526 |
| 1000.0 | 90.0° | 312.908 | 0.6258 | 687.09 | 1.2448 |
| 1000.0 | 90.0° | 335.606 | 0.6712 | 664.39 | 1.2089 |
| 1000.0 | 90.0° | 359.951 | 0.7199 | 640.05 | 1.1692 |
| 1000.0 | 90.0° | 386.061 | 0.7721 | 613.94 | 1.1250 |
| 1000.0 | 90.0° | 414.066 | 0.8281 | 585.93 | 1.0757 |
| 1000.0 | 90.0° | 444.101 | 0.8882 | 555.90 | 1.0200 |
| 1100.0 | 60.0° | 469.374 | 0.5163 | 630.63 | 1.2461 |
| 1100.0 | 60.0° | 503.421 | 0.5538 | 596.58 | 1.2047 |
| 1100.0 | 60.0° | 539.939 | 0.5939 | 560.06 | 1.1587 |
| 1100.0 | 60.0° | 579.106 | 0.6370 | 520.89 | 1.1072 |
| 1100.0 | 60.0° | 621.113 | 0.6832 | 478.89 | 1.0491 |
| 1100.0 | 60.0° | 666.168 | 0.7328 | 433.83 | 0.9831 |
| 1100.0 | 60.0° | 714.491 | 0.7859 | 385.51 | 0.9069 |
| 1100.0 | 60.0° | 766.320 | 0.8430 | 333.68 | 0.8173 |
| 1100.0 | 60.0° | 821.908 | 0.9041 | 278.09 | 0.7087 |
| 1200.0 | 15.0° | 799.492 | 0.0654 | 400.51 | 1.2535 |
| 1200.0 | 15.0° | 857.487 | 0.0701 | 342.51 | 1.2072 |
| 1200.0 | 15.0° | 919.688 | 0.0752 | 280.31 | 1.1556 |

Table 12: Table of Kinematics (Continued)

| $E_{\text{beam}}$ (MeV) | $\theta$ | $P_{\text{ref}}$ $(\text{MeV}/c)$ | $Q^2$ $(\text{GeV}^2)$ | $\omega$ (MeV) | $W$ $(\text{GeV}/c^2)$ |
|---|---|---|---|---|---|
| 1200.0 | 15.0° | 986.401 | 0.0807 | 213.60 | 1.0975 |
| 1200.0 | 15.0° | 1057.953 | 0.0865 | 142.05 | 1.0316 |
| 1200.0 | 15.0° | 1134.696 | 0.0928 | 65.30 | 0.9558 |
| 1200.0 | 60.0° | 538.099 | 0.6457 | 661.90 | 1.2175 |
| 1200.0 | 60.0° | 577.132 | 0.6926 | 622.87 | 1.1671 |
| 1200.0 | 60.0° | 618.997 | 0.7428 | 581.00 | 1.1104 |
| 1200.0 | 60.0° | 663.898 | 0.7967 | 536.10 | 1.0463 |
| 1200.0 | 60.0° | 712.057 | 0.8545 | 487.94 | 0.9729 |
| 1200.0 | 60.0° | 763.708 | 0.9164 | 436.29 | 0.8873 |
| 1200.0 | 60.0° | 819.107 | 0.9829 | 380.89 | 0.7853 |
| 1200.0 | 60.0° | 878.524 | 1.0542 | 321.48 | 0.6586 |
| 1600.0 | 15.0° | 1217.595 | 0.1328 | 382.40 | 1.2123 |
| 1600.0 | 15.0° | 1305.918 | 0.1424 | 294.08 | 1.1376 |
| 1600.0 | 15.0° | 1400.648 | 0.1527 | 199.35 | 1.0515 |
| 1600.0 | 15.0° | 1502.249 | 0.1638 | 97.75 | 0.9506 |
| 2000.0 | 15.0° | 1620.957 | 0.2209 | 379.04 | 1.1727 |
| 2000.0 | 15.0° | 1738.539 | 0.2370 | 261.46 | 1.0669 |
| 2000.0 | 15.0° | 1864.651 | 0.2541 | 135.35 | 0.9402 |
| 2400.0 | 15.0° | 1931.610 | 0.3159 | 468.39 | 1.2034 |
| 2400.0 | 15.0° | 2071.727 | 0.3388 | 328.27 | 1.0779 |
| 2400.0 | 15.0° | 2222.008 | 0.3634 | 177.99 | 0.9246 |
| 2800.0 | 15.0° | 2237.969 | 0.4270 | 562.03 | 1.2301 |
| 2800.0 | 15.0° | 2400.309 | 0.4580 | 399.69 | 1.0849 |
| 2800.0 | 15.0° | 2574.425 | 0.4912 | 225.57 | 0.9036 |
| 3200.0 | 15.0° | 2540.122 | 0.5539 | 659.88 | 1.2531 |
| 3200.0 | 15.0° | 2724.380 | 0.5941 | 475.62 | 1.0880 |
| 3200.0 | 15.0° | 2922.003 | 0.6372 | 278.00 | 0.8769 |
| 3600.0 | 15.0° | 3044.032 | 0.7468 | 555.97 | 1.0872 |
| 3600.0 | 15.0° | 3264.843 | 0.8010 | 335.16 | 0.8442 |
| 4000.0 | 15.0° | 3603.040 | 0.9822 | 396.96 | 0.8048 |

Table 13: Table of Kinematics (Continued)

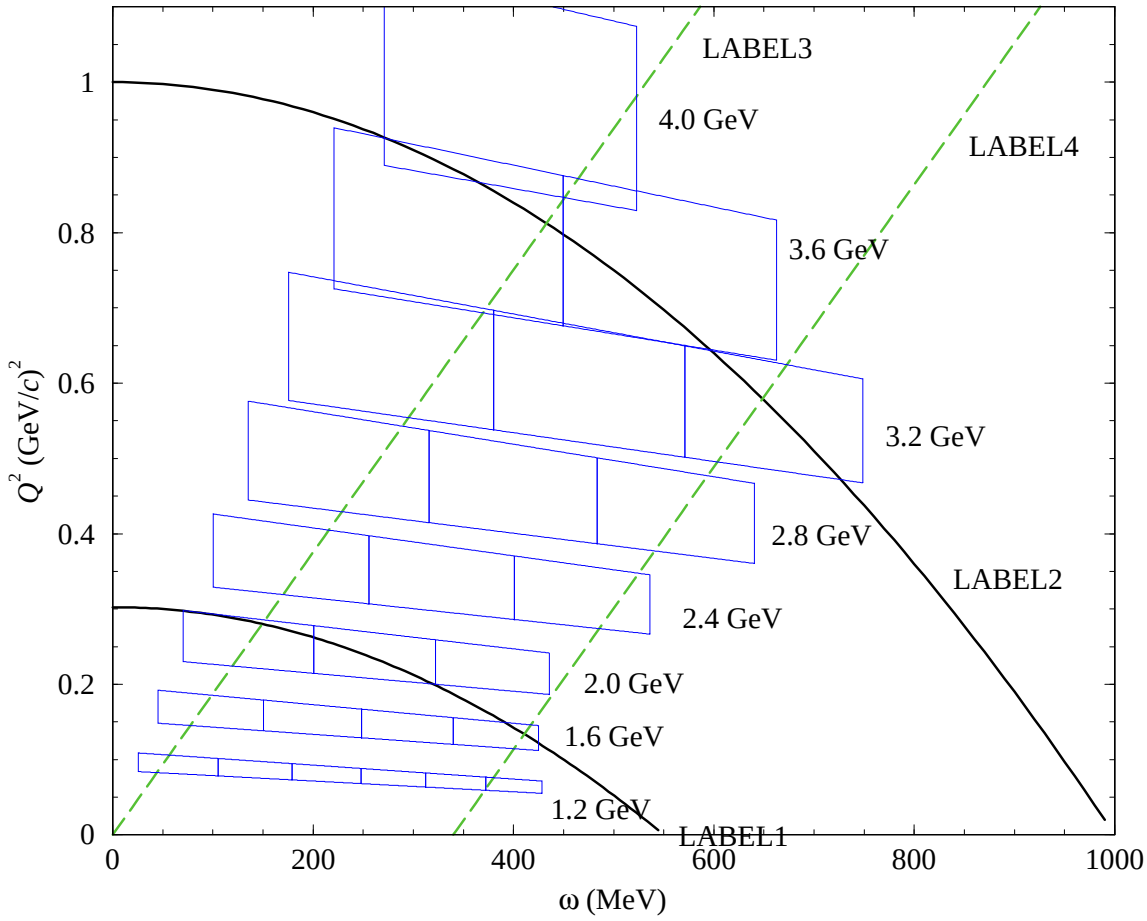


Figure 2: Kinematic coverage at 15°. The two solid lines correspond to $|\mathbf{q}| = 550$ MeV/$c$(lower one) and $1000$ MeV/$c$ (upper one). The two dashed lines correspond to $W = 940$ MeV/$c^2$ (left, quasi-elastic peak) and $1232$ MeV/$c^2$ (right, $\Delta$ resonance). Each box represents the actual acceptance of the spectrometer at each individual momentum setting. Corresponding beam energies are also specified.

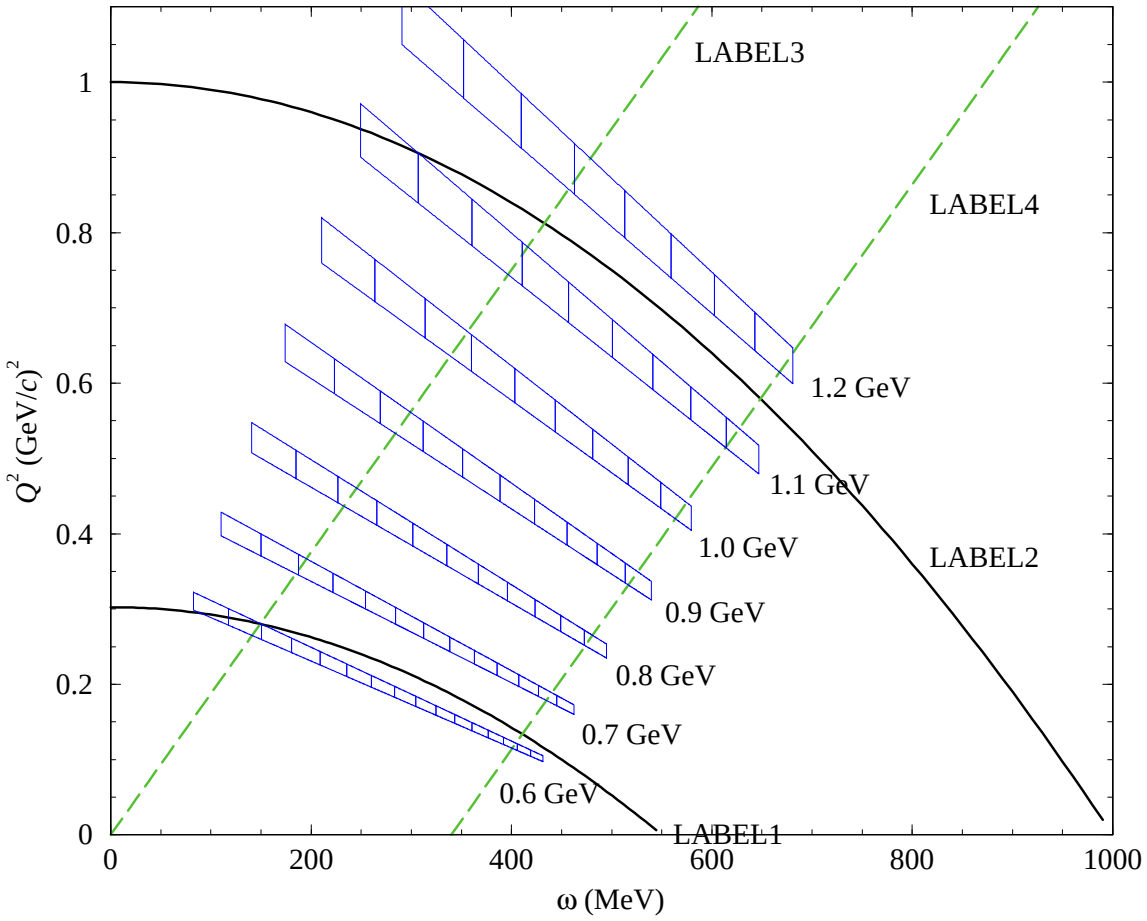


Figure 3: Kinematic coverage at 60°. The two solid lines correspond to $|\mathbf{q}| = 550$ MeV/$c$(lower one) and $1000$ MeV/$c$ (upper one). The two dashed lines correspond to $W = 940$ MeV/$c^2$ (left, quasi-elastic peak) and $1232$ MeV/$c^2$ (right, $\Delta$ resonance). Each box represents the actual acceptance of the spectrometer at each individual momentum setting. Corresponding beam energies are also specified.

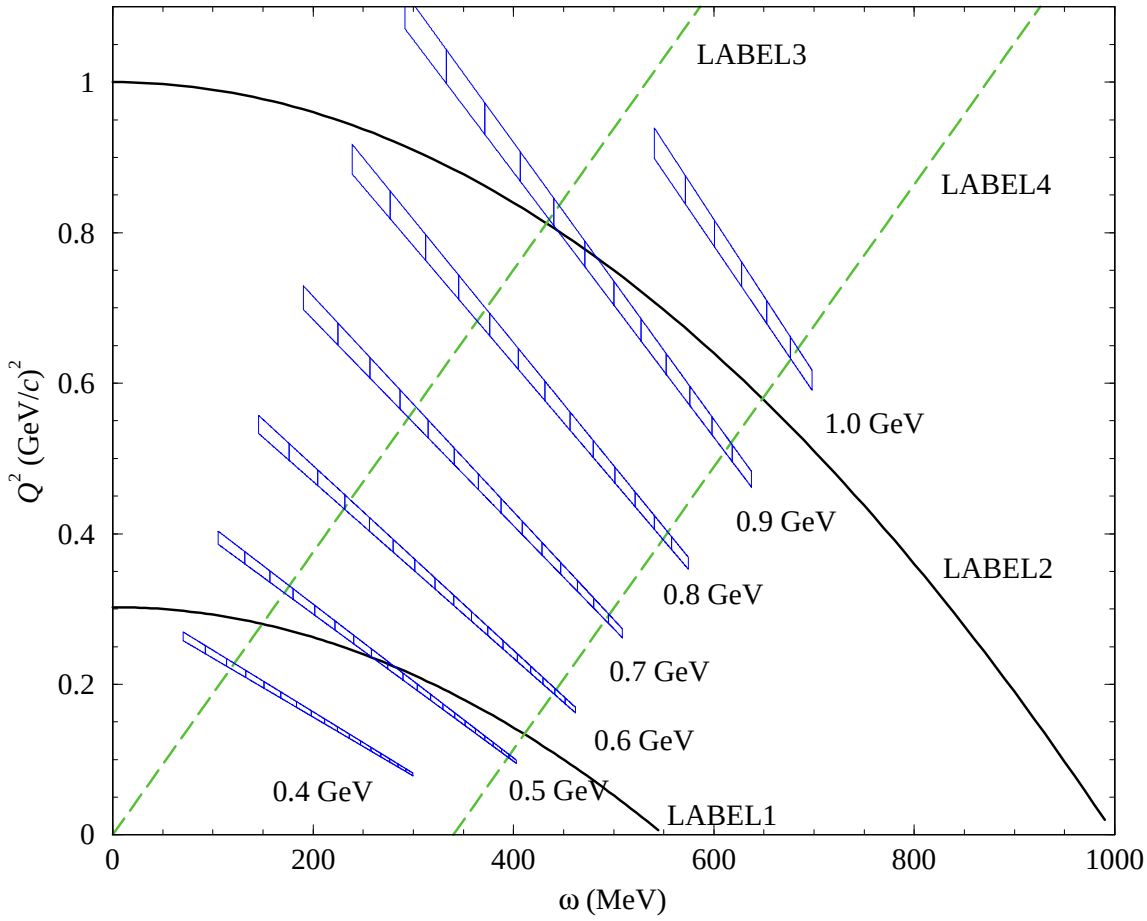


Figure 4: Kinematic coverage at 90°. The two solid lines correspond to $|\mathbf{q}| = 550$ MeV/$c$(lower one) and $1000$ MeV/$c$ (upper one). The two dashed lines correspond to $W = 940$ MeV/$c^2$ (left, quasi-elastic peak) and $1232$ MeV/$c^2$ (right, $\Delta$ resonance). Each box represents the actual acceptance of the spectrometer at each individual momentum setting. Corresponding beam energies are also specified.

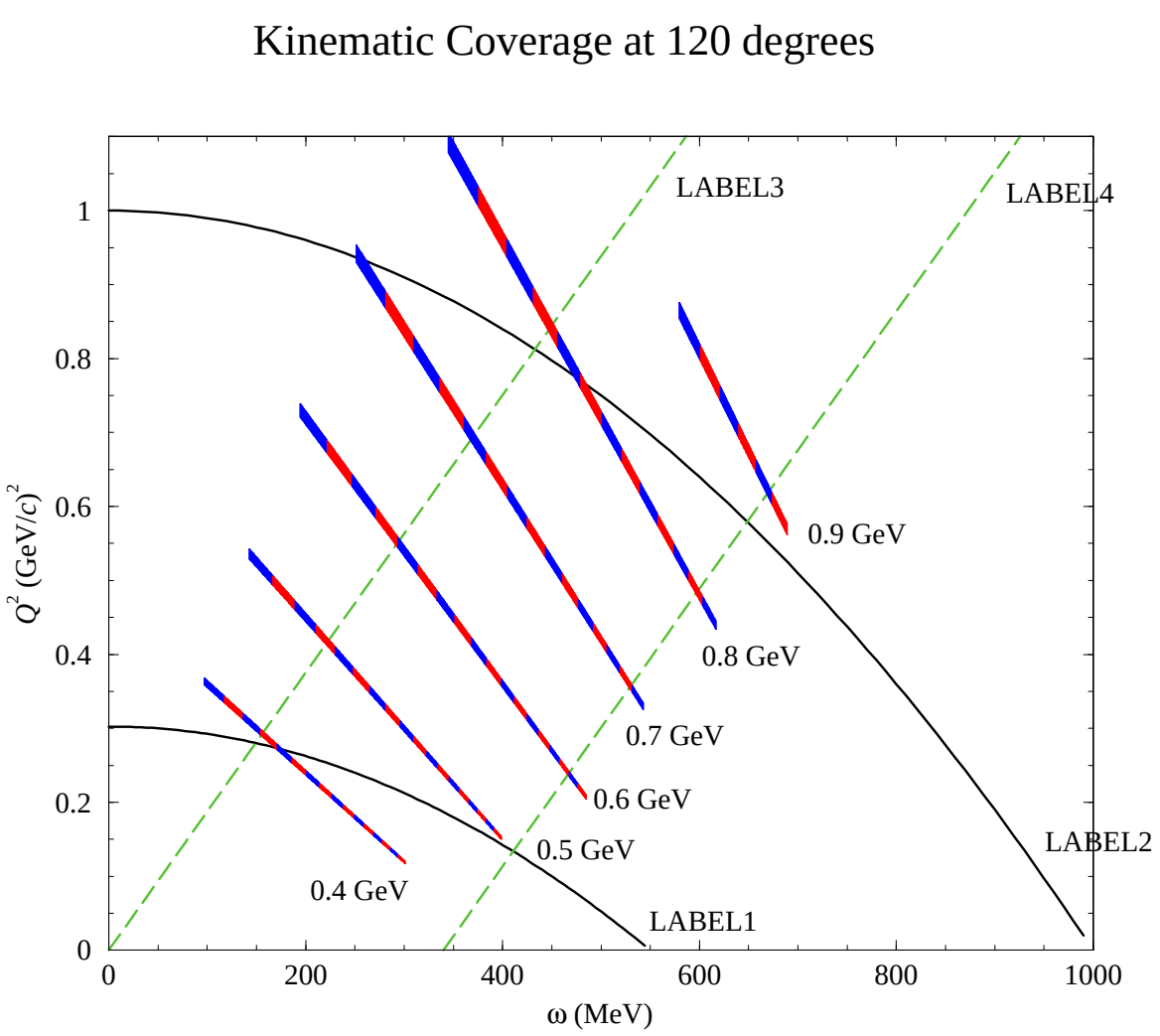


Figure 5: Kinematic coverage at 120°. The two solid lines correspond to $|\mathbf{q}| = 550$ MeV/$c$(lower one) and $1000$ MeV/$c$ (upper one). The two dashed lines correspond to $W = 940$ MeV/$c^2$ (left, quasi-elastic peak) and $1232$ MeV/$c^2$ (right, $\Delta$ resonance). Each box represents the actual acceptance of the spectrometer at each individual momentum setting. Corresponding beam energies are also specified.

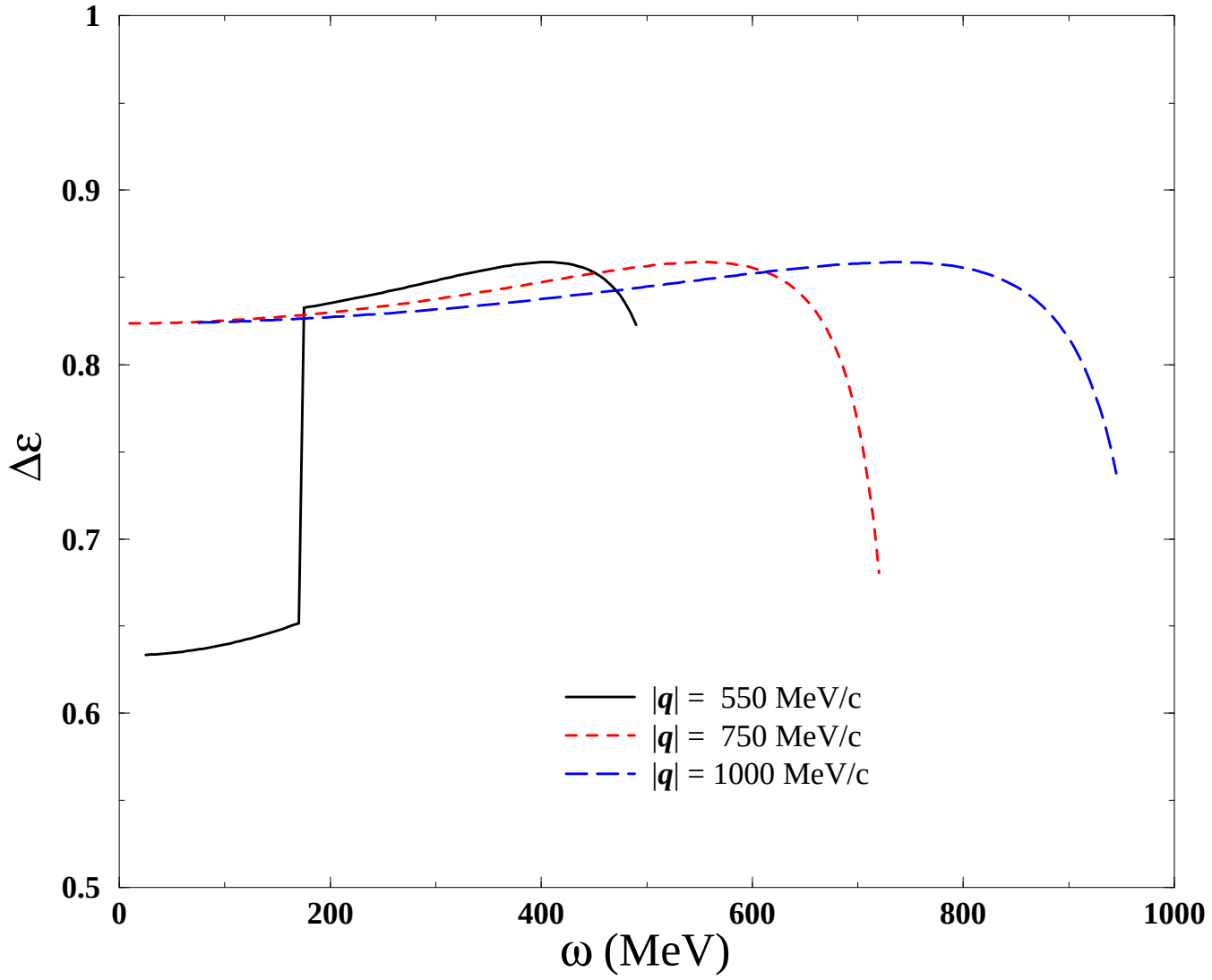


Figure 6: $\Delta\varepsilon$ achievable at Jefferson Lab for three values of $|\mathbf{q}|$.

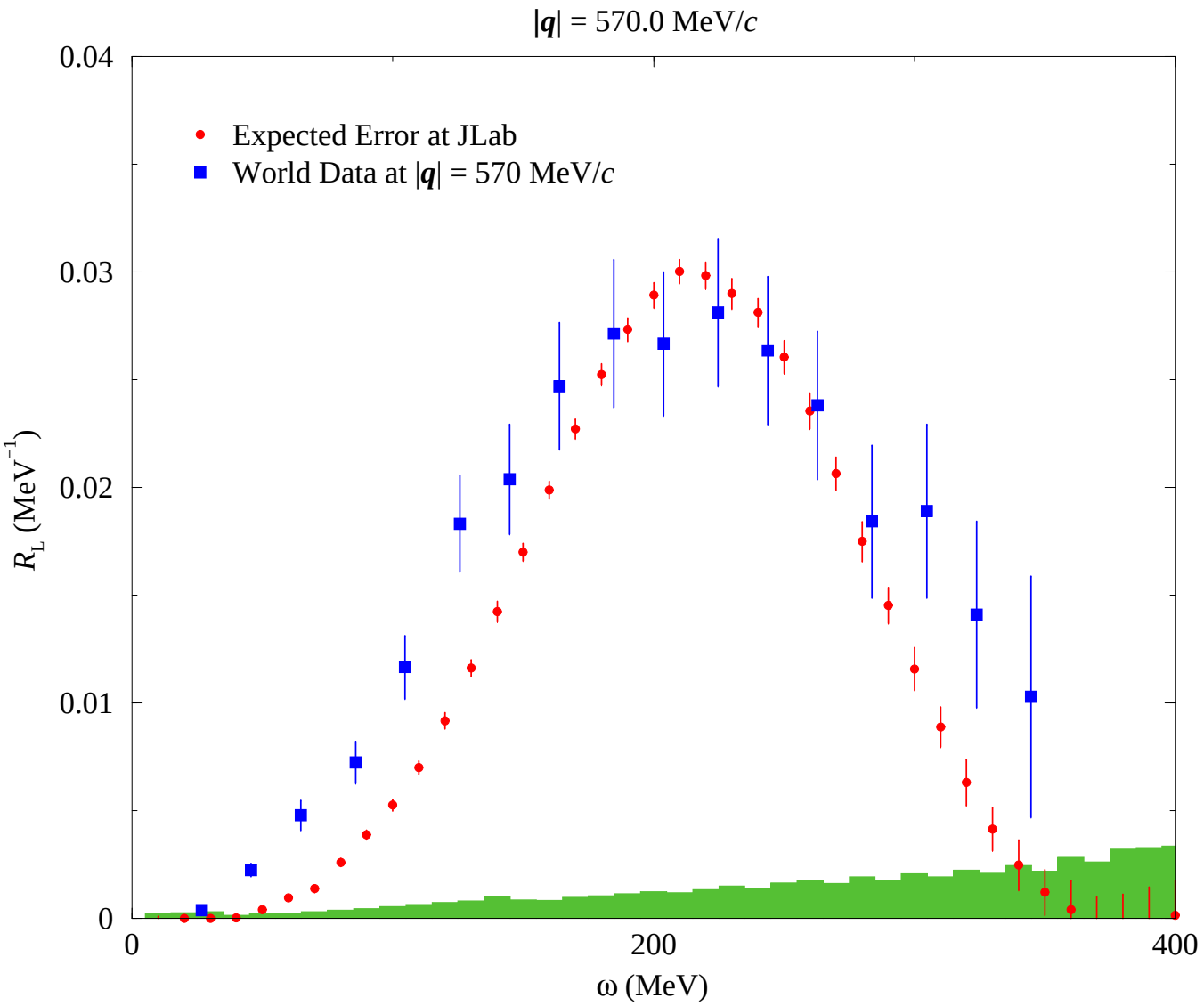


Figure 7: Comparison of expected statistical uncertainty on $R_L$ from Jefferson Lab with the world data at $|\mathbf{q}| = 570$ MeV/$c$. The error bars for the world data are statistical only. The band at the horizontal axis represents estimated systematic uncertainties.

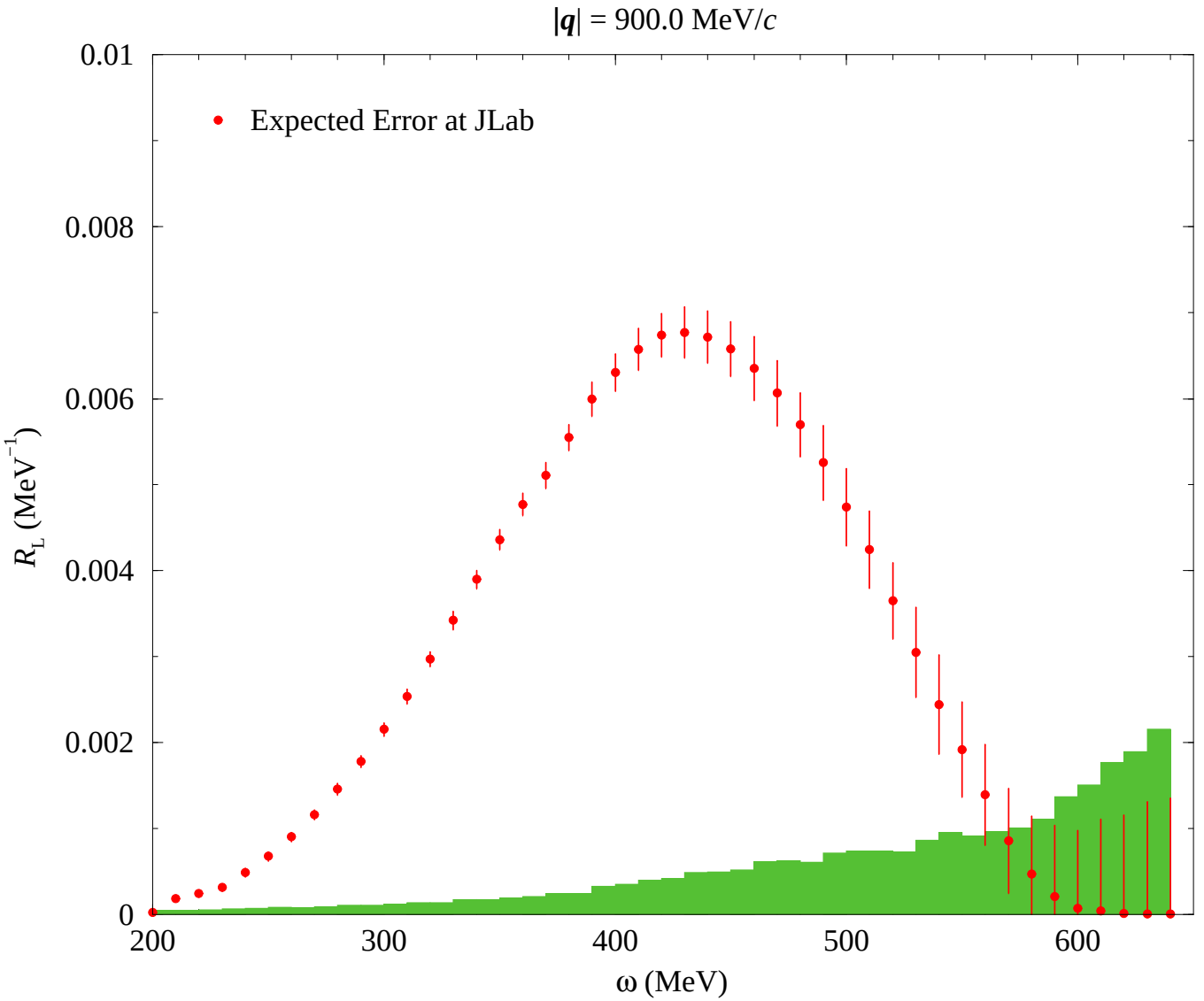


Figure 8: Expected statistical uncertainty on $R_L$ from Jefferson Lab at $|\mathbf{q}| = 900\,\mathrm{MeV}/c$. The band at the horizontal axis represents estimated systematic uncertainties.

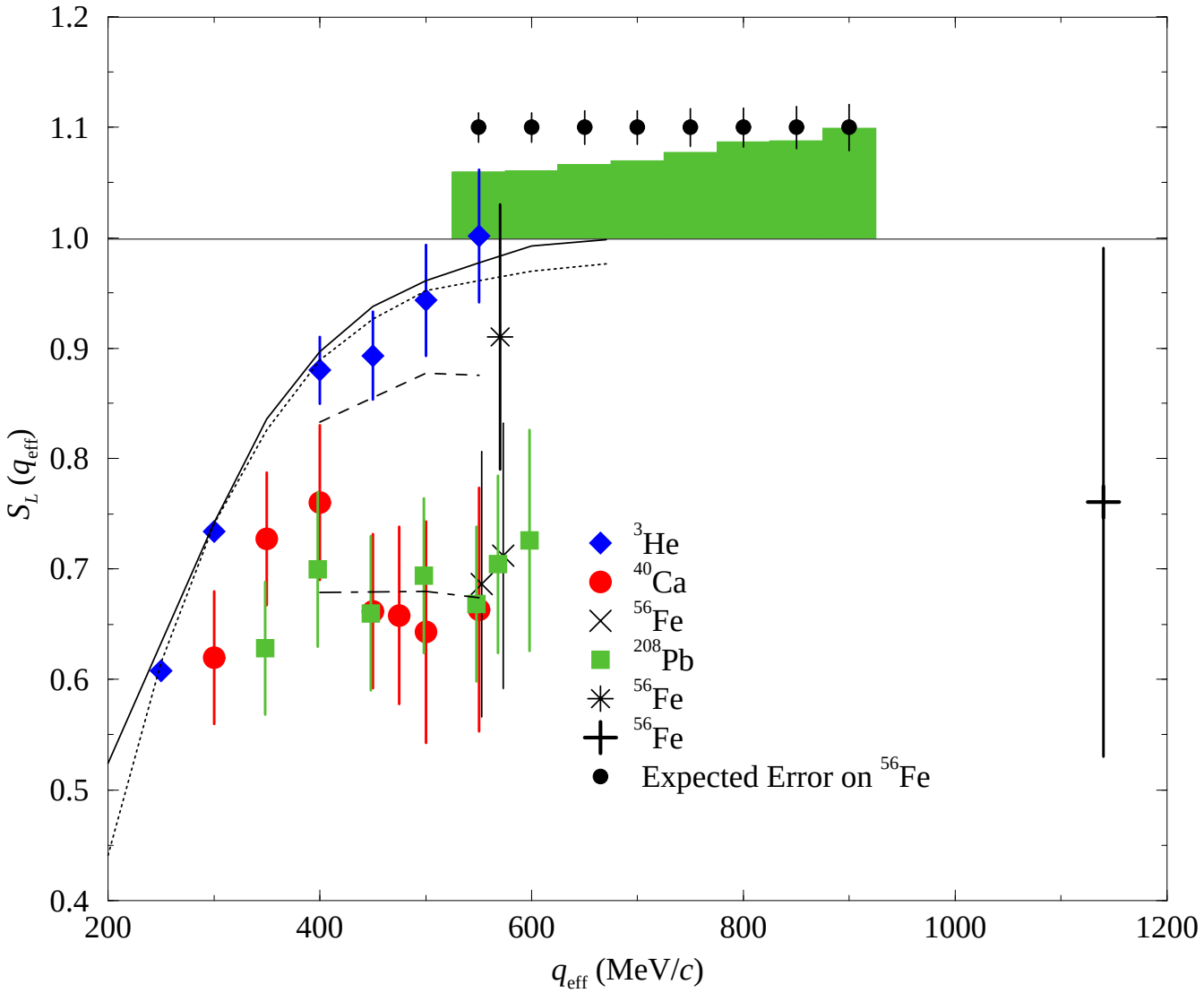


Figure 9: Comparison of expected statistical uncertainty on the Coulomb Sum from Jefferson Lab with the world data. Horizontal band represents estimated systematic uncertainties.